The Rise and Fall of the Natural Interest Rate*

Gabriele Fiorentini
Università di Firenze

Alessandro Galesi
Banco de España

Gabriel Pérez-Quirós
European Central Bank and CEPR

Enrique Sentana
CEMFI

October 2019

Abstract

We document a rise and fall of the natural interest rate (r^*) for several advanced economies, which starts increasing in the 1960's and peaks around the end of the 1980's. We reach this conclusion after showing that the Laubach and Williams (2003) model cannot estimate r^* accurately when either the IS curve or the Phillips curve is flat. In those empirically relevant situations, a local level specification for the observed interest rate can precisely estimate r^*. An estimated Panel ECM suggests that the temporary demographic effect of the young baby-boomers mostly accounts for the rise and fall.

JEL Codes: E43, E52, C18, C32
Keywords: Natural rate of interest, Kalman filter, Observability, Demographics

*We would like to thank Yunus Aksoy, Óscar Arce, Henrique S. Basso, Jesús Fernández-Villaverde, Juan Francisco Jimeno, Danilo Leiva-León, Galo Nuño, Carlos Thomas, and audiences at Banco de España, Banca d'Italia, European Central Bank, Center for Latin American Monetary Studies, the 42nd Symposium of the Spanish Economic Association (Barcelona), the 2017 Econometric Society European Winter Meeting (Barcelona), the 2nd Workshop on Macroeconomic and Financial Time Series Analysis (Lancaster, UK), the 15th International Conference in Economic Policy and Theory (Bilbao), the Czech National Bank Conference "The Future of Monetary Policy: What Can We See As the Dust Has Settled" (Prague), the Joint DNB/ECB Workshop on the Natural Rate of Interest (Amsterdam), and members of the "Natural Interest Rate" team of the Eurosystem Working Group on Econometric Modelling (WGEM) for very useful comments and suggestions. Disclaimer: The views expressed herein are those of the authors and not necessarily those of Banco de España or the Eurosystem. Email: fiorentini@disia.uinifi.it (Fiorentini), alessandro.galesi@bde.es (Galesi), Gabriel.Perez_Quiros@ecb.europa.eu (Pérez-Quirós), sentana@cemfi.es (Sentana).

1 Introduction

At the current juncture, interest rates are historically low in most advanced economies. This fact has led many economists to put forward the proposition that the *natural interest rate* (r^*), which is the rate that equates savings and investment and closes the output gap, has been falling over time. But given that the natural interest rate is a theoretical concept, it has to be measured from data. Since the seminal work of Laubach and Williams (2003, hereinafter LW2003), many papers have studied the measurement of this rate, showing that it has dramatically fallen over recent decades in tandem with a slowdown in growth (see for example Holston et al. 2017, hereinafter HLW2017). At the same time, the common perception is that the usual measures of r^* are generally imprecise and that the associated uncertainty could prevent the practical use of the estimated natural interest rate in policy applications.[1]

We contribute to this debate by first shedding light on the fundamental source of uncertainty that plagues the workhorse model of LW2003. In particular, we show that their model is generally able to produce very accurate estimates of r^*. However, the precision of their estimates dramatically falls when either the output gap is insensitive to the real interest rate gap (*flat IS curve*), or inflation is insensitive to the output gap (*flat Phillips curve*).[2] In those cases, it is not possible to uniquely identify the unobserved growth and non-growth components of r^* from the data. Unfortunately, those two cases are empirically relevant according to a wide set of estimates reported in the existing literature.

We show that an augmented version of the LW2003 model, which assumes the stationarity of the interest rate gap, can identify both components of r^* even when the IS and Phillips curves are flat. Our assumption also allows us to identify r^* using a univariate local level specification which decomposes the observed real rate into its permanent and transitory components, where the former closes the interest rate gap and stabilizes the

[1]See for example Clark and Kozicki (2005), Weber et al. (2008), as well as recent papers by Hamilton et al. (2016), Taylor and Wieland (2016), and Beyer and Wieland (2019)

[2]In the following, we extensively use the definition of real interest rate gap introduced by Neiss and Nelson (2003), as the spread between the actual and natural levels of the real interest rate.

output gap and inflation. When we apply this alternative specification to historical data spanning more than a century for a set of advanced economies, we document a generalized decline of the natural interest rate since the start of the twentieth century until the 1960's, followed by a *rise and fall*, with a peak around the end of the 1980's. Since the local level model is silent about the determinants of the estimated r^*, we shed some light on why this rise and fall occurred by estimating a Panel Error Correction Model (ECM) using a set of indicators as potential drivers of r^*. Our results provide suggestive evidence that the rise and fall of r^* could be attributed to the post-war baby boom, which generated a temporary rise of the population share of young workers.

As we have already mentioned, the natural interest rate is not directly observable because according to the definition by Woodford (2003), it represents the real interest rate which would be observed in a full employment economy without nominal rigidities. For this reason, empirical researchers have employed a variety of approaches to measure it.[3] The popular approach introduced in LW2003 consists of a semi-structural econometric model whose equations are inspired by the key equations of the New Keynesian framework. Specifically, their model consists of two main equations: an aggregate demand equation (IS curve), which states that the gap between the observed real interest rate and the natural interest rate affects the output gap; and an aggregate supply equation (Phillips curve), which relates inflation to the output gap. The model is closed by assuming that the natural interest rate is the sum of two unobserved nonstationary components: the underlying trend growth of the economy, and a bundle of other factors unrelated to growth (the so-called z component). However, the uncertainty surrounding the estimated natural interest rate is very large, as pointed out not only by LW2003 but also by several subsequent studies which have estimated their model or its variants.[4]

We dig into the mechanics of the LW2003 model and show that it is generally able to

[3] The methods used in the literature cover time series models such as in Crespo Cuaresma et al. (2004), Cour-Thimann et al. (2006), Lubik and Matthes (2015), and Hamilton et al. (2016), full-fledged structural macroeconomic models like the estimated DSGE in Giammarioli and Valla (2003), and more recently in Barsky et al. (2014), Cúrdia et al. (2015), Del Negro et al. (2017), and Gerali and Neri (2018), and financial frameworks such as the dynamic term structure models estimated in Christensen and Rudebush (2017). We refer to Brand et al. (2018) for a complete review of the different approaches.

[4] See for instance Clark and Kozicki (2005), Kiley (2015), Beyer and Wieland, (2019), Lewis and Vazquez-Grande (2019), HLW2017.

produce very accurate estimates of r^*. However, the precision of the model drops in two specific circumstances. First, when the IS curve is flat. In that case, the output gap is insensitive to the real interest rate gap, so that information about the output gap cannot identify the non-growth component of the natural interest rate which affects the interest rate gap. Second, when the Phillips curve is flat. In this other case, inflation is insensitive to the output gap, so the former variable can identify neither the output gap nor potential output. As a consequence, it is not possible to separately identify potential output from the non-growth component of the natural interest rate.

In more technical terms, the model is said to be unobservable in those cases in which it is not possible to uniquely identify the natural interest rate from the available data. Originally introduced by Kalman (1960), observability is a fundamental concept of modern control system theory. It measures the ability to infer the internal state variables of a dynamic system given knowledge of the external outputs. In the context of linear time-invariant systems, observability can be evaluated by checking the rank of the observability matrix.[5] The key intuition for this rank condition is that the problem of determining the path of the state vector in a linear system can be simplified to the problem of finding its initial condition: once we know it, we can recover the full path of the state variables given the transition equation and knowledge of the disturbances.

Unfortunately, the slopes of the IS and Phillips curves estimated in the literature tend to be close to 0. This fact was already documented in LW2003 using data for the United States, and has been confirmed in several empirical papers which estimate their model for a number of advanced economies, as reported in Table 3 in the Appendix. In those circumstances, the LW2003 model is close to failing the observability condition, which implies a very imprecisely estimated natural interest rate driven by large uncertainty of the filter rather than the parameters.

To solve this problem, we start from the observation that the LW2003 model treats the observed real interest rate as exogenous, therefore leaving the dynamic process for the interest rate gap undefined. But as soon as one imposes the stationarity of the interest rate gap, we show that one can identify both the growth and non-growth components of

[5] See for example Harvey (1989) for a precise definition, as well as the examples in the Appendix.

r^* even when the IS and Phillips curves are flat. The extra identification restriction comes from the fact that the observed real rate can be decomposed into a transitory component (interest rate gap) and a permanent component (the natural rate). A direct implication of our result is that, if a researcher is interested in estimating r^* but not necessarily its growth and non-growth components, then a valid alternative is to estimate a univariate local level model (see Harvey, 1989), which decomposes the observed real interest rate into its permanent and transitory components. Thus, the rationale behind our approach is that the interest rate gap is the stationary deviation between the observed rate and its unobserved permanent component. Hence, the interest rate gap can be closed if and only if the observed real interest rate coincides with its permanent component. Moreover, under a general class of New Keynesian models, output gap and inflation get completely stabilized by setting the interest rate gap to zero on a period-by-period basis. For this reason, we can think of the permanent component of the observed real interest rate as a measure of r^*.

Still, the local level model cannot identify the growth and non-growth components of r^* because it exploits data on the interest rate only. Nevertheless, given that the augmented model is observable, it is robust to situations in which the empirical estimates suggest flat IS and Phillips curves. Perhaps more importantly, when we apply our proposed approach to post-war U.S. data, the local level specification produces a precise estimate of r^* while the LW2003 model is close to unobservable.

Next, we collect historical data at annual frequency over the period 1891-2016 for a set of seventeen advanced economies. Such a sample is likely to produce flat IS and Phillips curves for two reasons: (*i*) the low frequency of the annual data may be too coarse to identify any relation among output gap, interest rate gap, and inflation; and (*ii*) the long time span may imply structural breaks in the relationships among variables. For those reasons, we estimate the natural interest rate of each economy, thereby using international data to externally validate our local level specification. We find a common decline in r^* across countries since the start of the twentieth century until the 1960's. We also find a subsequent statistically significant rise and fall, which peaks around the end of the 1980's. Importantly, this rise and fall is already visible in the actual data on real interest rates across countries. Jordà et al. (2019) also document a rise and fall in the real safe rate, pointing out that, from a long-run perspective, the relevant question is why the safe rate was so high in the mid-1980s, rather than why it has declined so much since then.

Finally, we explore the reasons behind the documented rise and fall. As we have mentioned before, the local level model, which uses data on real interest rates only, is silent about the drivers of r^*. However, by exploiting the cross-country variation of the estimated r^* we document a large synchronization of natural rates. Interestingly, we also find that countries which feature larger falls in the natural rate since the 1990's are also those for which the rate increased more over the period 1960's – 1980's. This evidence suggests that both the rise and the fall of r^* may be the result of a common set of drivers, and that any explanation that seeks to explain the recent fall in interest rates should also be consistent with explaining the precedent rise. We shed some light on this issue by estimating a Panel ECM which postulates a long-run relationship between the observed real interest rate and a set of indicators. The intuition is that, if there exists a long-run relation among the unobserved natural rate and its drivers, then it should also hold among the observable counterparts. The real interest rate predicted by the model can thus be used as a proxy for the natural interest rate. In this respect, we show that the Panel ECM predicts a rate which closely follows the r^* estimated by the local level model.

Data availability and endogeneity concerns limit our analysis to a relatively small set of plausibly exogenous drivers of r^*: productivity growth, demographic composition, and a measure of risk. Through the lens of the model, productivity growth plays a negligible role in driving the rise and fall of the natural rate of interest. Specifically, we document a tenuous link of productivity growth with the real interest rate, thus complementing results in Lunsford and West (2019) for the United States. This result also supports those studies that have emphasized a tenuous link between trend growth of the economy and the real interest rate, such as Clark and Kozicki (2005) for the United States, and Hamilton et al. (2016), who used historical data for a large set of OECD economies. In contrast, we find that risk is related to important developments in r^*, and more specifically, that it accounts for a substantial part of the fall since the 1990's. This result is in line with Gerali and Neri (2018), who find that risk premium shocks have reduced the natural rate in both the United States and the euro area. In this respect, our results are in line with Del Negro et al. (2017), according to whom the safety and liquidity premia have negatively affected the U.S. natural interest rate. Last, but not least, we find that the changing demographic composition accounts for the bulk of the rise and fall in the natural interest rate. Specifically, the rise can be explained by the post-war baby boom, which temporarily increased the share of young workers in the population. Once the baby boom ends, the share of young workers goes back to its previous negatively trended path, which in turn leads to a process of population ageing. This finding provides empirical support to recent studies which have emphasized the role of demographics for the evolution of the real interest rate (Aksoy et al. 2019; Carvalho et al. 2016; Favero et al. 2016a, 2016b; Gagnon et al. 2016; Lisack et al. 2017; Ferrero et al. 2019; Rachel and Smith, 2017).

The rest of the paper is organized as follows. In section 2, we study the cases under which the LW2003 model fails to accurately estimate r^*. Then, in section 3, we introduce our alternative approach for estimating r^*, which we apply to historical international data. Finally, we present our conclusions in section 4. Auxiliary results are gathered in appendices.

2 Why is the Uncertainty on r^* so Large?

In this section we document the large uncertainty surrounding the estimated natural interest rate by estimating the HLW2017 model, which is a recent version of the LW2003 framework, using data for the United States. In particular, we show that the large imprecision mostly stems from the uncertainty in the filter. To understand why filter uncertainty may be so large, we dig into the mechanics of the model and study its observability properties. We show two cases in which the model cannot recover the unobserved natural interest rate given the data: (*i*) if the output gap is insensitive to the interest rate gap (*flat IS curve*); and (*ii*) if inflation is insensitive to the output gap (*flat Phillips curve*). These cases are empirically relevant, according to estimates found in the literature. This implies that the model is close to being unobservable, which means that the unobserved natural rate can barely be recovered, and only with large filter uncertainty.

2.1 Uncertainty in the Holston, Laubach, and Williams Model

The building block of the model consists of two main equations

$$\tilde{y}_t = \alpha_{y,1}\tilde{y}_{t-1} + \alpha_{y,2}\tilde{y}_{t-2} - \gamma(r_{t-1} - r^*_{t-1}) + \varepsilon^{\tilde{y}}_t, \tag{1}$$

$$\pi_t = \alpha_\pi \pi_{t-1} + (1-\alpha_\pi)\pi_{t-2,4} + \kappa\tilde{y}_{t-1} + \varepsilon^{\pi}_t, \tag{2}$$

where the aggregate demand equation in (1) posits that the output gap $\tilde{y}_t$, defined as the deviation of the (log-) real GDP, y_t, from its unobserved potential level, y^*_t, depends on its own lags and past realizations of the real interest rate gap, defined as the deviation of the observed real interest rate, r_t, from the natural interest rate. In turn, the aggregate supply equation in (2) links the observed inflation rate, π_t, to its own lag, to the average of its second to fourth lags, $\pi_{t-2,4}$, and to the lagged output gap. There are two serially and mutually uncorrelated shocks, $\varepsilon^{\tilde{y}}_t$ and ε^{π}_t, which affect the output gap and inflation respectively, whose variances are denoted by $\sigma^2_{\tilde{y}}$ and σ^2_π.

In turn, the unobserved natural interest rate depends on two unobserved processes,

$$r^*_t = 4g_t + z_t, \tag{3}$$

where $4g_t$ is the annualized growth of the economy, and z_t is a process which captures other determinants unrelated to growth. The unobserved processes follow the laws of motion given by

$$y^*_t = y^*_{t-1} + g_{t-1} + \varepsilon^{y^*}_t, \tag{4}$$

$$g_t = g_{t-1} + \varepsilon^{g}_t, \tag{5}$$

$$z_t = z_{t-1} + \varepsilon^{z}_t, \tag{6}$$

where equation (4) defines the law of motion of potential output, which depends on its past lag and on lagged trend growth of the economy, g_{t-1}. In turn, equations (5) and (6) state that the trend growth of the economy and the z_t component follow random walk processes. There are three serially and mutually uncorrelated disturbances, $\varepsilon^{y^*}_t$, ε^{g}_t, and ε^{z}_t, whose respective variances are $\sigma^2_{y^*}$, σ^2_g, and σ^2_z. Given this specification, the (log-) real

GDP and its potential level are integrated processes of order 2, while the natural rate of interest is I(1), being the sum of two random walk processes.

The model can be cast in state-space form and the estimation of parameters and unobserved states can be done through the application of the standard Kalman filter. When estimating the model, LW2003 encountered a so-called *pile-up problem*, whereby the estimated variances of the innovations to the nonstationary processes z_t and g_t have point mass at zero even though their true values are positive (see Stock, 1994, and Laubach, 2001). To avoid this problem, HLW2017 employ an estimation method which proceeds in sequential steps. The first step consists in estimating a simpler model to recover a measure of potential output, which omits the real rate gap term from equation (1) and assumes that the trend growth rate is constant. The Stock and Watson's (1998) median unbiased estimator of $\lambda_g = \frac{\sigma_g}{\sigma_{y^*}}$ is obtained by testing for a structural break with unknown break date in equation (4). The second step amounts to imposing the estimated value of λ_g from the first step, followed by the inclusion of the real interest rate gap in the output gap equation under the assumption that z_t is constant. Again, the Stock and Watson's (1998) median unbiased estimator of $\lambda_z = \frac{\gamma\sigma_z}{\sigma_{\tilde{y}}}$ is obtained by testing for a structural break with unknown break date on the IS curve of equation (1). The third and final step consists of imposing the estimated value of λ_g from the first step and λ_z from the second step, and estimating the full model by Maximum Likelihood. We report the procedure in detail in the Appendix.

Following this approach, we estimate the model using U.S. quarterly data over the period 1960Q3-2016Q3. We compute confidence intervals using Hamilton's (1986) Monte Carlo procedure that accounts for both filter and parameter uncertainty, whose details we provide in the Appendix. Figure 1 reports the estimated r^* jointly with 90% probability bands. As can be seen, the natural rate has declined over time. Nevertheless, it is estimated with large imprecision, as already emphasized by LW2003, as well as in more recent studies.[6]

[6] See for instance Clark and Kozicki (2005), Kiley (2015), Beyer and Wieland (2019), Lewis and Vazquez-Grande (2019), and HLW2017.

Figure 1: U.S. natural rate of the HLW model: estimate and 90% bands

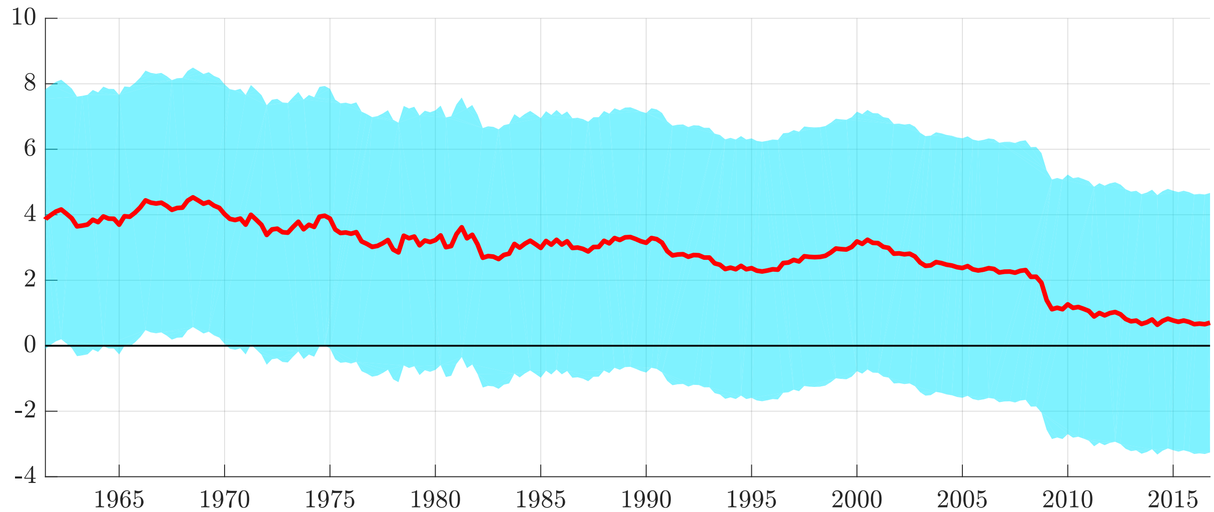

Notes: quarterly data, 1961Q2-2016Q3. Estimated r^* jointly with 90% confidence bands. Bands reflect both filter and parameter uncertainty, and are computed using Hamilton's (1986) approach with 2000 Montecarlo replications of the parameter vector.

The question that we pose is: why is uncertainty so large? Imprecise estimates could be either due to large *parameter uncertainty*, because the true values of the parameters are unknown and therefore they are estimated with some error, or due to *filter uncertainty*, because the realizations of the state vector are also unknown. To quantify the relative importance of uncertainty on the filter and on the parameters, we recompute the bands as follows: to isolate the role of filter uncertainty, we compute the bands without accounting for parameter uncertainty as detailed in the Appendix, and vice versa for assessing the role of parameter uncertainty. The results of this exercise are reported in Figure 2, which plots the estimated r^* and 90% confidence bands, which reflect either parameter uncertainty in panel (a), or filter uncertainty in panel (b). Uncertainty stemming from the filter is dramatically larger than parameter uncertainty, which suggests that filter uncertainty is the reason why the natural rate gets imprecisely estimated.

Figure 2: Filter and parameter uncertainty in the HLW model

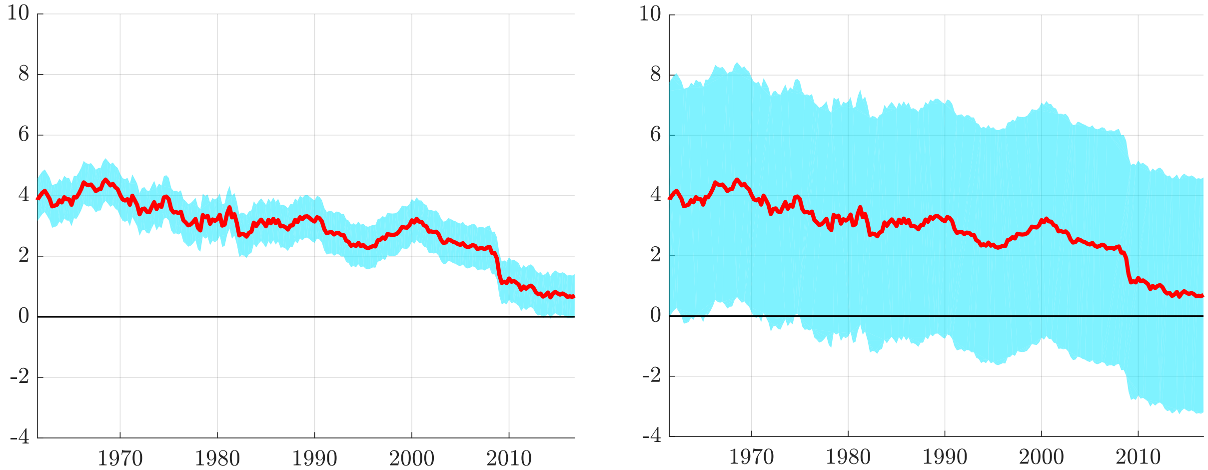

(a) Parameter uncertainty

(b) Filter uncertainty

Notes: quarterly data, 1961Q2-2016Q3. Estimated r^* jointly with 90% confidence bands. Bands in the left-hand side chart reflect parameter uncertainty; bands in the right-hand side reflect filter uncertainty. Bands are computed using Hamilton's (1986) approach with 2000 replications on the parameter vector.

According to equation (3), the natural interest rate is defined as the sum of two components: (i) the (annualised) trend growth of the economy; and (ii) the z_t process, which captures all other factors besides growth that could affect the natural rate. Importantly, both components are unobserved and therefore will be estimated with error. We compute bands associated to filter uncertainty for these two components. Figure 3 plots the estimates for the trend growth and the z_t process, where bands are computed by considering just the uncertainty on the filter. Filter uncertainty associated with the trend growth is relatively small compared to the one of the z_t component, whose bands are markedly larger.

Figure 3: Filter uncertainty in the HLW model: components of r^*

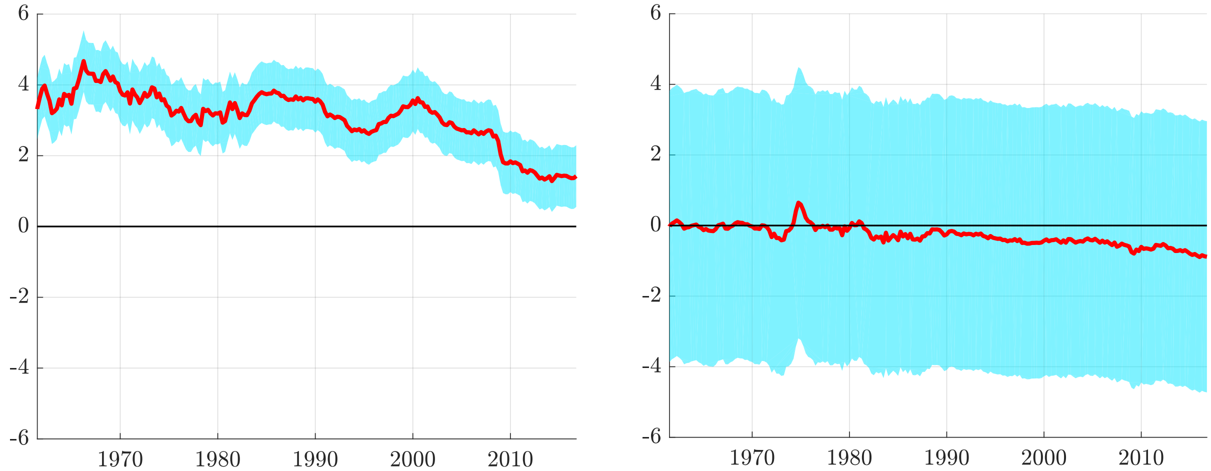

(a) Trend growth (b) Other factors

Notes: quarterly data, 1961Q2-2016Q3. Estimated annualised trend growth and z_t component jointly with 90% confidence bands. Bands in the left-hand side chart reflect filter uncertainty associated to annualised trend growth; bands in the right-hand side reflect filter uncertainty associated to the z_t component.

So in summary, the natural interest rate of the HLW model is very imprecisely estimated, mainly because one of its components, the z_t process, is imprecisely estimated too. But what drives the large imprecision of the z_t component? To shed light on this question, in the rest of the section we provide an in-depth analysis of the structure of the HLW model, which will help us understand under which circumstances the model fails to work correctly. To do so, we resort to the notion of *observability* introduced by Kalman (1960), a fundamental concept of modern control system theory which measures the ability to precisely infer the inner states of a system given the available data.

2.2 Observability in the Holston, Laubach, and Williams Model

Consider the following state-space representation of the HLW model, in which the measurement equation is given by

$$\begin{bmatrix} y_t \\ \pi_t \end{bmatrix} = \underbrace{\begin{bmatrix} 1-\alpha_y & 1+4\gamma & \gamma \\ -\kappa & 0 & 0 \end{bmatrix}}_{\mathbf{Z}} \begin{bmatrix} y^*_{t-1} \\ g_{t-1} \\ z_{t-1} \end{bmatrix} + \underbrace{\begin{bmatrix} \alpha_y & 0 & 0 & -\gamma \\ \kappa & \alpha_\pi & 1-\alpha_\pi & 0 \end{bmatrix}}_{\mathbf{D}} \begin{bmatrix} y_{t-1} \\ \pi_{t-1} \\ \pi_{t-2|4} \\ r_{t-1} \end{bmatrix} + \begin{bmatrix} \varepsilon^{\tilde{y}}_t + \varepsilon^{y^*}_t \\ \varepsilon^{\pi}_t \end{bmatrix},$$

where for ease of exposition we have assumed that only one lag of the output gap enters the right-hand side of the IS curve.[7] In turn, the transition equation reads

$$\begin{bmatrix} y_t^* \\ g_t \\ z_t \end{bmatrix} = \underbrace{\begin{bmatrix} 1 & 1 & 0 \\ 0 & 1 & 0 \\ 0 & 0 & 1 \end{bmatrix}}_{\mathbf{T}} \begin{bmatrix} y_{t-1}^* \\ g_{t-1} \\ z_{t-1} \end{bmatrix} + \begin{bmatrix} \varepsilon_t^{y^*} \\ \varepsilon_t^g \\ \varepsilon_t^z \end{bmatrix}.$$

The model posits that two endogenous observables, y_t and π_t, are linked through the $\mathbf{Z}$ matrix to three unobserved states given by potential output, y^*, trend growth, g, and other factors which may affect the natural rate, z. Finally, the unobserved states evolve over time according to the transition matrix $\mathbf{T}$.[8]

Suppose that the particular values of all system matrices are known with certainty, as well as the realizations of the disturbances. In this context, we ask the question: can we learn about the dynamic behavior of the vector of unobserved states by using information about all the observables and disturbances? The key condition which allows the state vector to be determined exactly is that the system should be *observable*. In the context of linear systems, a necessary condition for the system to be observable is that the rank of the *observability matrix* is equal to the number of unobserved states; see for example Harvey (1989). Specifically, the observability matrix of a linear system with s unobserved states is given by

$$\mathbf{O} \equiv \begin{bmatrix} \mathbf{Z} \\ \mathbf{ZT} \\ \mathbf{ZT}^2 \\ \vdots \\ \mathbf{ZT}^{s-1} \end{bmatrix}, \tag{7}$$

and the system is observable if Rank $(\mathbf{O}) = s$. Details on the derivation of this condition

[7] By having just one lag of the output gap, we are able to obtain a minimal state space representation of the model which features just three unobserved states. Nevertheless, we report in the Appendix a more complex case with two lags that provides the same results.

[8] This specific state space representation introduces some non-zero correlation across disturbances of the measurement and state equations, $\mathbf{u}_t$ and $\mathbf{v}_t$. This representation is a minimal realisation, that is, it minimizes the length of the state vector, and it helps in deriving analytical results. Nonetheless, the specific choice of the state space representation does not change results in terms of observability of the original model, as we discuss in the Appendix. Moreover, when estimating the HLW model, we employ a different state space form according to which the disturbances $\mathbf{u}_t$ and $\mathbf{v}_t$ are uncorrelated; see details in the Appendix. In any event, when the measurement and transition equation disturbances are correlated, one can still employ an appropriately modified Kalman filter by following the steps in Harvey (1989, chap. 3).

are in the Appendix. In the HLW model, in particular, the observability matrix reads

$$\mathbf{O} = \begin{bmatrix} \mathbf{Z} \\ \mathbf{ZT} \\ \mathbf{ZT}^2 \end{bmatrix} = \begin{bmatrix} 1-\alpha_y & 1+4\gamma & \gamma \\ -\kappa & 0 & 0 \\ 1-\alpha_y & 2+4\gamma-\alpha_y & \gamma \\ -\kappa & -\kappa & 0 \\ 1-\alpha_y & 3+4\gamma-2\alpha_y & \gamma \\ -\kappa & -2\kappa & 0 \end{bmatrix}. \tag{8}$$

Therefore, the rank of the observability matrix depends on three model parameters: (i) the coefficient of the lagged output gap in the IS curve, α_y; (ii) the sensitivity of inflation to past output gap, κ; and (iii) the parameter governing the sensitivity of the output gap to the real rate gap, γ. If the rank of $\mathbf{O}$ in (8) is less than three, which is the number of unobserved states, then some elements of the state vector are unrecoverable by the data. By inspecting the observability matrix, we can easily find two cases of rank deficiency:

Case 1. The IS curve is flat ($\gamma = 0$)

If the elasticity of current output gap to past real interest rate gap is zero, then the IS curve is flat. In that case, the observability matrix becomes

$$\mathbf{O} = \begin{bmatrix} 1-\alpha_y & 1 & 0 \\ -\kappa & 0 & 0 \\ 1-\alpha_y & 2-\alpha_y & 0 \\ -\kappa & -\kappa & 0 \\ 1-\alpha_y & 3-2\alpha_y & 0 \\ -\kappa & -2\kappa & 0 \end{bmatrix},$$

and the third column, which is associated to the z_t process, reduces to a vector of zeros. Therefore, in this case $\text{Rank}(\mathbf{O}) < 3$ and the model is not observable. In particular, it is not possible to recover the path for the z_t process. Since the output gap is insensitive to the real interest rate gap, data on the output gap do not provide information to identify the z_t process, which is a component of the natural interest rate. We can still uniquely determine the paths for potential output and trend growth, as long as either the Phillips curve is not flat ($\kappa \neq 0$) or the autoregressive coefficient of the output gap satisfies $|\alpha_y| < 1$.

Case 2. The Phillips curve is flat ($\kappa = 0$)

If the elasticity of current inflation to past output gap is zero, the Phillips curve is flat.

Then, the observability matrix becomes

$$\mathbf{O} = \begin{bmatrix} 1-\alpha_y & 1+4\gamma & \gamma \\ 0 & 0 & 0 \\ 1-\alpha_y & 2+4\gamma-\alpha_y & \gamma \\ 0 & 0 & 0 \\ 1-\alpha_y & 3+4\gamma-2\alpha_y & \gamma \\ 0 & 0 & 0 \end{bmatrix},$$

and we can observe that the first and third columns are linearly dependent, with the third column equal to $\gamma/(1-\alpha_y)$ times the first column. This implies that it is not possible to separately identify potential output from the z_t component, while it is still possible to identify the process for the underlying trend growth. Therefore, Rank($\mathbf{O}$) < 3, and the model is not observable either.

Thus, we have provided two examples in which the HLW model fails to meet the required observability condition: (*i*) *Flat IS curve:* the sensitivity of the output gap to the real interest rate gap is zero ($\gamma = 0$); and (*ii*) *Flat Phillips curve:* the sensitivity of inflation to the output gap is zero ($\kappa = 0$).[9] Now the question is: what do the data tell us about the magnitude of these sensitivities? Figure 4 reports the frequencies of estimates of γ and κ across several studies that estimate the LW2003 model or variants of it using data for several advanced economies. Table 3 reports further details about these estimates. As can be seen, the estimated sensitivities are very small and close to zero, so very flat IS and Phillips curves seem to be more the rule than the exception.

[9] This result holds also when considering a more complex model in which two lags of the output gap appear in the IS curve, as shown in the Appendix. Moreover, if the z_t component is assumed to be stationary, the model is still unobservable when the IS curve is flat ($\gamma = 0$), but it becomes observable when the Phillips curve is flat ($\kappa = 0$), provided, of course, that the IS curve is not flat ($\gamma \neq 0$). We report further details in the Appendix.

Figure 4: Steepness of IS and Phillips curves: estimates in the literature

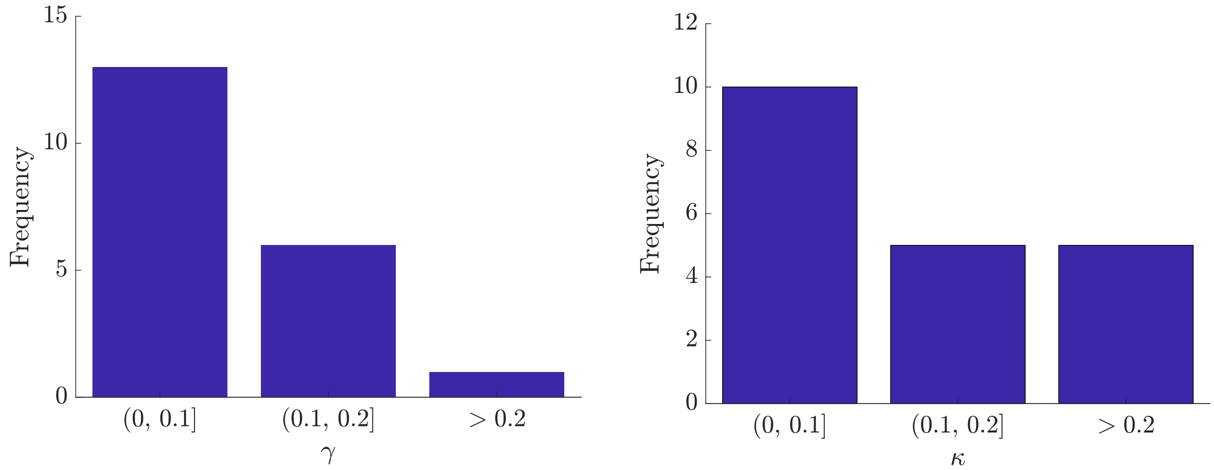

Notes: Frequency of estimates of γ and κ across studies as reported in Table 3 in the Appendix. γ and κ measure the steepness of the IS and Phillips curves, respectively.

To study the practical implications of the lack of observability, we consider the mean squared error matrix of the state vector,

$$\mathbf{P}_{t|t-1} \equiv E\left[\left(\mathbf{x}_t - \hat{\mathbf{x}}_{t|t-1}\right)\left(\mathbf{x}_t - \hat{\mathbf{x}}_{t|t-1}\right)'\right],$$

where $\hat{\mathbf{x}}_{t|t-1}$ is the one-sided filtered estimate of the state vector. Next, we calculate the stationary matrix using the estimated parameters for the United States and the prediction and updating equations,

$$\begin{aligned} \mathbf{P}_{t|t-1} &= \mathbf{T}\mathbf{P}_{t-1|t-1}\mathbf{T}' + \mathbf{R}\mathbf{Q}\mathbf{R}', \qquad t = 1, \ldots, T \\ \mathbf{P}_{t|t} &= \mathbf{P}_{t|t-1} - \mathbf{P}_{t|t-1}\mathbf{Z}'\mathbf{F}_t^{-1}\mathbf{Z}\mathbf{P}_{t|t-1}, \end{aligned}$$

where $\mathbf{F}_t = \mathbf{Z}\mathbf{P}_{t|t-1}\mathbf{Z}' + \mathbf{H}$, setting a diffuse prior for $\mathbf{P}_{0|0}$. Finally, we compute the filter variance of the natural rate and its components over a grid of values for γ and κ, with the remaining parameters set to the estimated values reported in Table 2.

Figure 5: Filter uncertainty and slopes of the IS and Phillips curves

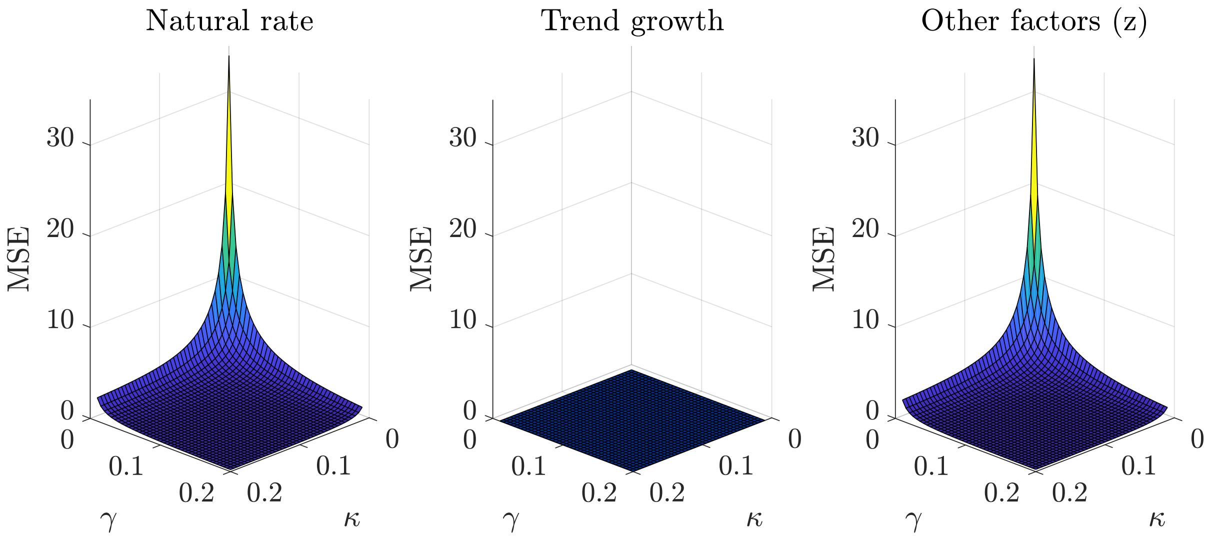

Notes: mean squared error of the unobserved states as a function of γ and κ, where γ and κ measure the steepness of the IS and Phillips curves, respectively.

Figure 5 reports the mean squared error of the unobserved states as a function of γ and κ. Filter uncertainty associated to the natural interest rate is small for large values of γ and κ. Given that we have previously shown that the bulk of the imprecision in the HLW model is due to filter uncertainty, we can conclude that for substantially large values of those sensitivities, the HLW model precisely estimates r^*. However, when either γ or κ approaches zero, the uncertainty associated with r^* dramatically increases, mostly because of the rise in the uncertainty associated with the z_t component. As we have mentioned before, z_t is the component which affects the uncertainty of the natural interest rate the most, while the process for trend growth features relatively small uncertainty regardless of the values of γ and κ.

3 An Alternative Approach to Extract r^*

3.1 A Local Level Model for the Real Interest Rate

We have shown that the HLW model imprecisely estimates the natural interest rate when the IS and the Phillips curves are close to being flat, because the model is close to being unobservable in those circumstances. How can we the precisely estimate r^*? To answer this question, we start from the observation that the HLW model treats the observed interest rate, r_t, as an exogenous variable which determines the interest rate gap of the IS equation in (1). Given the exogeneity of the observed real rate, the dynamic properties of the gap between the observed rate and the natural rate are unknown, as well as the dynamics of the output gap in equation (1). In practical terms, the HLW model does not guarantee that either the interest rate gap or the output gap are stationary. In what follows, we explore the observability properties of an alternative version of the HLW model which explicitly restricts the two gaps to be stationary.

Specifically, we augment the original HLW model by adding an equation which defines the real interest rate gap, $\tilde{r}_t$, as the stationary deviation between the real rate from its unobserved permanent component,

$$\tilde{r}_t = r_t - r_t^*, \tag{9}$$

where the natural interest rate, r^*, is defined in equation (3). For simplicity of exposition, we assume that the interest rate gap follows the stationary AR(1) process

$$\tilde{r}_t = \alpha_r \tilde{r}_{t-1} + \varepsilon_t^{\tilde{r}}, \tag{10}$$

with $|\alpha_r| < 1$, and $\varepsilon_t^{\tilde{r}}$ is a white-noise disturbance, uncorrelated with the other shocks of the model, whose variance is $\sigma_{\tilde{r}}^2$.

This augmented version of the HLW model can also be written in state-space form, with the measurement equation given by

$$\begin{bmatrix} y_t \\ \pi_t \\ r_t \end{bmatrix} = \underbrace{\begin{bmatrix} 1-\alpha_y & 1+4\gamma & \gamma \\ -\kappa & 0 & 0 \\ 0 & 4(1-\alpha_r) & 1-\alpha_r \end{bmatrix}}_{\mathbf{Z}} \begin{bmatrix} y_{t-1}^* \\ g_{t-1} \\ z_{t-1} \end{bmatrix} +$$

$$+ \underbrace{\begin{bmatrix} \alpha_y & 0 & 0 & -\gamma \\ \kappa & \alpha_\pi & 1-\alpha_\pi & 0 \\ 0 & 0 & 0 & \alpha_r \end{bmatrix}}_{\mathbf{D}} \begin{bmatrix} y_{t-1} \\ \pi_{t-1} \\ \pi_{t-2|4} \\ r_{t-1} \end{bmatrix} + \begin{bmatrix} \varepsilon_t^{\tilde{y}} + \varepsilon_t^{y^*} \\ \varepsilon_t^{\pi} \\ 4\varepsilon_t^{g} + \varepsilon_t^{z} + \varepsilon_t^{\tilde{r}} \end{bmatrix},$$

where, once again we have assumed for simplicity that only one lag of the output gap enters the right-hand side of the IS curve. The key difference with respect to the structure of the original HLW model is that the observed real rate is now endogenous, and it depends on the unobserved states through the $\mathbf{Z}$ matrix. In contrast, the transition equation is essentially unchanged with respect to the standard HLW model, being given by

$$\begin{bmatrix} y_t^* \\ g_t \\ z_t \end{bmatrix} = \underbrace{\begin{bmatrix} 1 & 1 & 0 \\ 0 & 1 & 0 \\ 0 & 0 & 1 \end{bmatrix}}_{\mathbf{T}} \begin{bmatrix} y_{t-1}^* \\ g_{t-1} \\ z_{t-1} \end{bmatrix} + \begin{bmatrix} \varepsilon_t^{y^*} \\ \varepsilon_t^{g} \\ \varepsilon_t^{z} \end{bmatrix}.$$

The observability of the augmented HLW model now depends on the rank of the matrix

$$\mathbf{O} = \begin{bmatrix} \mathbf{Z} \\ \mathbf{ZT} \\ \mathbf{ZT}^2 \end{bmatrix} = \begin{bmatrix} 1-\alpha_y & 1+4\gamma & \gamma \\ -\kappa & 0 & 0 \\ 0 & 4(1-\alpha_r) & 1-\alpha_r \\ 1-\alpha_y & 2+4\gamma-\alpha_y & \gamma \\ -\kappa & -\kappa & 0 \\ 0 & 4(1-\alpha_r) & 1-\alpha_r \\ 1-\alpha_y & 3+4\gamma-2\alpha_y & \gamma \\ -\kappa & -2\kappa & 0 \\ 0 & 4(1-\alpha_r) & 1-\alpha_r \end{bmatrix}. \tag{11}$$

Compared to the observability matrix of the original HLW model in (8), this matrix includes three additional rows (the third, the sixth, and the ninth), which also depend on the autoregressive coefficient of the interest rate gap, α_r. Since the interest rate gap is stationary, $|\alpha_r| < 1$, those three rows are nonzero and they help to identify the unobserved states of the model. To illustrate our claim, suppose that both Phillips and IS curves are flat, so that $\gamma = 0$ and $\kappa = 0$. In this extreme case the observability matrix in (11) becomes

$$\mathbf{O} = \begin{bmatrix} 1-\alpha_y & 1 & 0 \\ 0 & 0 & 0 \\ 0 & 4(1-\alpha_r) & 1-\alpha_r \\ 1-\alpha_y & 2-\alpha_y & 0 \\ 0 & 0 & 0 \\ 0 & 4(1-\alpha_r) & 1-\alpha_r \\ 1-\alpha_y & 3-2\alpha_y & 0 \\ 0 & 0 & 0 \\ 0 & 4(1-\alpha_r) & 1-\alpha_r \end{bmatrix}.$$

Importantly, the third column, which is associated to the z_t process, is a nonzero linearly independent vector when the interest rate gap is stationary, $|\alpha_r| < 1$, so that it is possible to recover the path for the z_t process. More generally, as long as both the interest rate gap and the output gap are stationary, $\text{Rank}(\mathbf{O}) = 3$, so all unobserved states can be recovered from the data. Notice that if the interest rate gap were nonstationary, the process for the observed real interest rate would be the sum of two unobserved nonstationary processes, the natural interest rate and the rate gap, which would not be separately identifiable. In that particular case, the observability matrix in (11) would coincide with the one of the original HLW model in (8).

Therefore, it is possible to identify the natural interest rate even when both IS and Phillips curves are flat under the assumption that the interest rate gap is stationary. The identification restriction comes from the fact that the observed real rate is decomposed into a stationary component (the interest rate gap) and a nonstationary component (the natural rate).

Indeed, the natural rate of the HLW model is nonstationary and follows a random walk process. This can be easily seen by combining equations (3), (5) and (6), which yields

$$r_t^* = r_{t-1}^* + \varepsilon_t^{r^*} \qquad \varepsilon_t^{r^*} \sim N(0, \sigma_{r^*}^2), \tag{12}$$

where $\sigma_{r^*}^2 = 16\sigma_g^2 + \sigma_z^2$. This observation implies that if we are interested in estimating r^* but not necessarily its components, then we can resort to a univariate local level model (Harvey, 1989) based on equations (9), (10) and (12), which decomposes the observed real interest rate into its permanent and transitory components. In this setup, the interest rate gap can be closed if and only if the observed real rate coincides with its permanent component. In addition, for a general class of New Keynesian models, output gap and inflation get stabilized when the interest rate gap is zero. For example, consider the non-policy block of the model in Galí (2008, chap. 3),

$$\tilde{y}_t = E_t\left[\tilde{y}_{t+1}\right] - \gamma \tilde{r}_t, \tag{13}$$

$$\pi_t = \beta E_t\left[\pi_{t+1}\right] + \kappa \tilde{y}_t, \tag{14}$$

which consists of the dynamic IS equation (13) and the New Keynesian Phillips curve

(14). We can solve the system composed by equations (13), (14) and (10) to obtain

$$\begin{aligned}\tilde{y}_t &= -\frac{\gamma\kappa}{(1-\alpha_r)(1-\alpha_r\beta)}\tilde{r}_t,\\ \pi_t &= -\frac{\gamma}{1-\alpha_r}\tilde{r}_t,\end{aligned}$$

so that both the output gap and inflation depend on the interest rate gap. By setting the real rate gap to zero period-by-period, both the output gap and inflation get completely stabilized. As a result, we can think of the permanent component, r_t^*, as a measure of the natural interest rate.

Compared to the standard HLW model, though, the local level model can always identify r^* but not its growth and non-growth components, because it exploits data on the real interest rate only. To see why, consider the observability matrix of the system implied by equations (9), (10) and (12),

$$\mathbf{O} = \begin{bmatrix} 1 & 1 \\ 1 & \alpha_r \end{bmatrix}.$$

In this context, it is possible to recover the two unobserved states (the natural interest rate and the interest rate gap) if the rank of the observability matrix is equal to two, which always happens given that the interest rate gap is restricted to be stationary. Therefore, the local level model provides a valid alternative to the HLW model in those cases in which the latter is almost unobservable, which happens when either the IS or Phillips curve is flat.

To confirm this point, we compute the filter uncertainty associated to the natural interest rate implied by the original HLW model, the augmented HLW model, and the local level model, for different degrees of steepness of the IS and Phillips curves.[10]

Figure 6 reports the mean squared error of r^* as a function of γ and κ for the HLW, augmented HLW, and local level models. When the IS and Phillips curves are relatively steep, all models feature small filter uncertainty. When both curves are close to being flat,

[10] As before, for each model we obtain the stationary mean squared error matrix of the state vector using the corresponding prediction and updating equations. For comparability across the models, parameters of system matrices are set to estimated values from the augmented HLW model. We then compute the MSE matrices for a grid of values for γ and κ, which are the parameters that measure the steepness of the IS and Phillips curves, respectively.

Figure 6: Filter uncertainty of r^* across different models

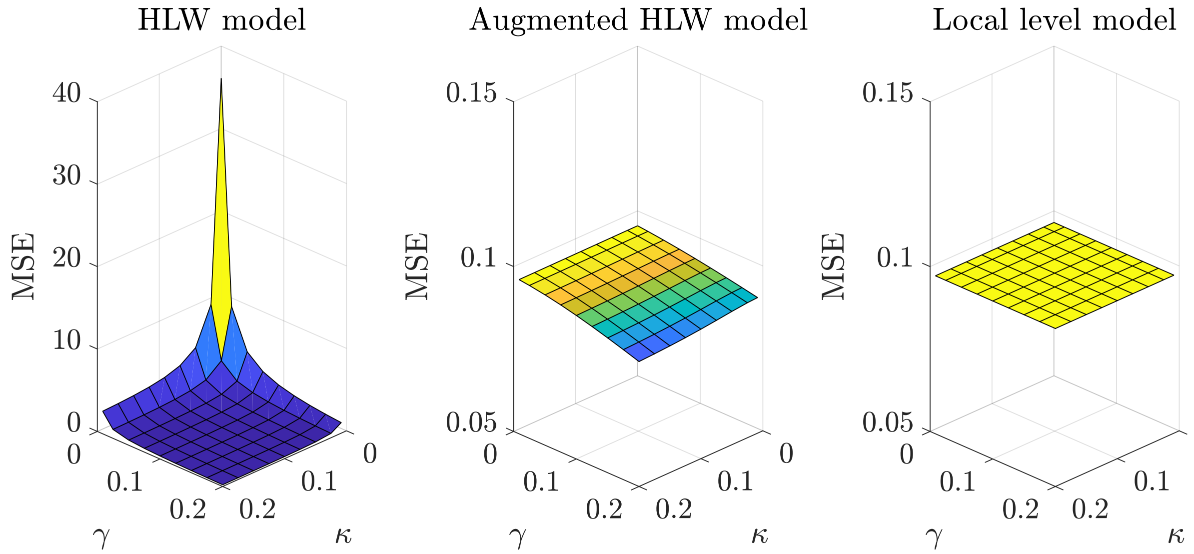

Notes: mean squared error associated with the natural interest rate, r^*, as a function of γ and κ, where γ and κ measure the steepness of the IS and Phillips curves, respectively.

in contrast the uncertainty implied by the HLW model dramatically increases, because the model get close to being unobservable. On the other hand, both the augmented HLW and local level models continue to feature very little uncertainty, which increases as γ and κ get close to zero in the case of the augmented HLW model, but which remains constant in the case of the local level model. Overall, both the augmented HLW model and the local level model are valid alternatives to the HLW model in those cases in which the observability of the latter is at stake. Therefore, both approaches may complement each other. For the specific purpose of our subsequent analysis, which spans more than one century of data, we opt for the local level model which is more robust to potential model misspecification, a key issue for the conduct of monetary policy frequently emphasized in the literature (see for instance Levin and Williams, 2003, or Orphanides and Williams, 2007).

To gauge the properties of the natural interest rate r^* extracted by the local level model, we use data on the U.S. ex-ante real interest rate as previously employed for the estimated HLW model. As in HLW2017, we solve any potential pile-up problem by first applying the Stock and Watson's (1998) median unbiased estimator of $\lambda_r = \frac{\sigma_{\tilde{r}}}{\sigma_{r^*}(1-\alpha_{\tilde{r}})}$,

Figure 7: U.S. natural rate estimates: HLW and local level models

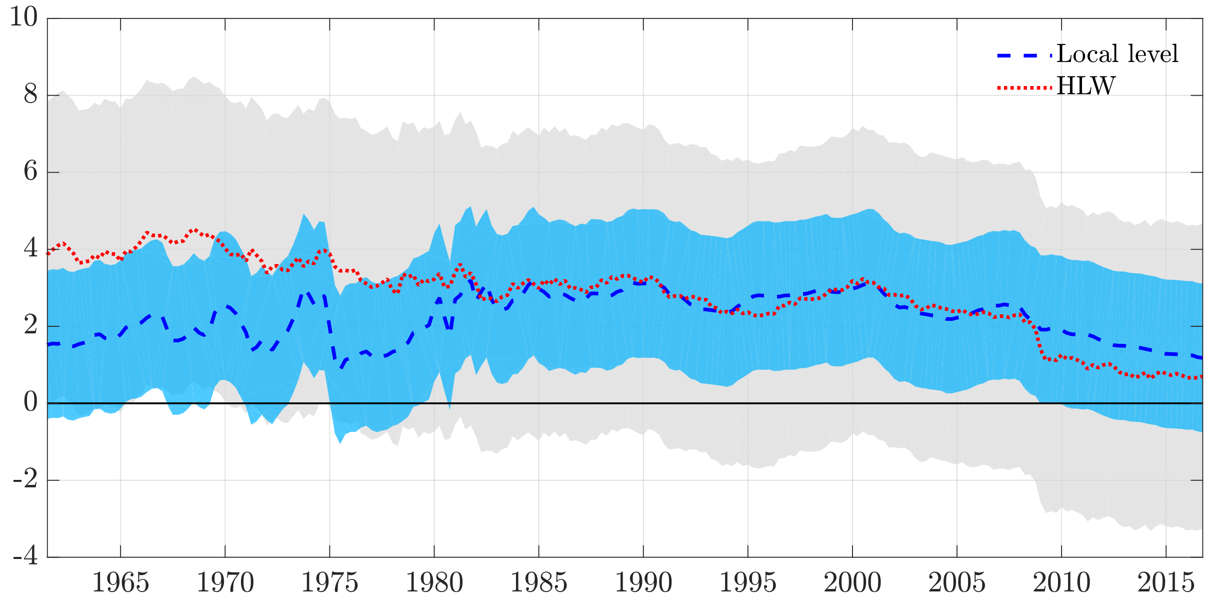

Notes: quarterly data, 1961Q2-2016Q3. Solid blue line refers to r^* estimated by the local level model. Dotted red line refers to r^* estimated by the HLW model. 90% confidence bands reflect both filter and parameter uncertainty, and are computed using Hamilton's (1986) approach with 2000 replications of the parameter vector.

and then estimating all remaining model parameters for given $\hat{\lambda}_r$. Finally, we compute confidence intervals using Hamilton's (1986) Monte Carlo procedure, which accounts for both filter and parameter uncertainty.

Figure 7 reports the estimated natural rate of interest obtained by the local level model, as well as the r^* obtained by the HLW model. By comparing bands across model estimates, we observe that the estimates of the local level model are relatively more precise than those of the HLW model. In this respect, Figure 18 in the Appendix confirms that the higher efficiency of the local level model is mostly attributable to lower filter uncertainty, and marginally to lower parameter uncertainty.

Both models predict a fall of the natural interest rate since the 1980's from roughly three percent to one percent. Interestingly though, while the HLW model predicts that prior to the 1980's the rate was also decreasing, the local level model predicts an increase from about 1.8 percent in 1960 to 3 percent in 1980. In the following we seek to understand to what extent this discrepancy is attributable to the lack of observability of the HLW model. As we have previously shown, the natural interest rate of the HLW model is very imprecisely estimated because one of its components, the z_t process, is imprecisely estimated too. In those circumstances, the initial condition of the unobserved z_t process, z_0, which is arbitrarily set in the estimation stage, may influence the estimated unobserved states of the model. In practice, there is no clear a priori on which value the initial condition z_0 should take, since the z process has not a directly observable counterpart. As in HLW2017, we have considered so far setting z_0 equal to zero, but now we estimate the model for a set of different arbitrary initial conditions $z_0 \in \{-5, -2, 0, 2, 5\}$.

Figure 8 reports the corresponding estimated the unobserved states. Panel (a) shows that the choice of the initial condition substantially affects the estimated path of the z_t process: while in the benchmark case with $z_0 = 0$, the z process witnesses a slow fall over the sample (ranging from 0% to about -1%), the fall dramatically increases when z_0 is set to 2$, and the path even changes direction and increases over time when z_0 is either set to -2% or -5%. Conversely, panel (b) shows that the path of the unobserved trend growth is relatively stable over different initial conditions, confirming our previous findings about this process being observable in the model. In turn, panel (c) shows that the resulting trajectory of the estimated natural interest rate is dramatically dependent on the choice of the initial condition for the z process.

Also the local level model requires setting an arbitrary initial condition for the unobserved natural interest rate, for which we have used so far the value of the actual real interest rate one quarter before the beginning of the estimation sample, which averages $r_0^* = 1.8\%$. We perform a similar sensitivity analysis by estimating the model for different initial conditions with $r_0^* \in \{-3.2\%, -0.2\%, 1.8\%, 3.8\%, 6.8\%\}$. Panel (d) of Figure 8 shows that the estimated natural interest rate is virtually unaffected by the initial condition since paths overlap, thus confirming that the observability of the local level model guarantees its robustness to different initial conditions for the unobserved r^*.

So in summary, the lack of observability in the HLW model not only implies a very imprecisely estimated r^*, but also a more worrying dependence of the estimate on the choice of the initial condition for the z process. Conversely the local level model, being by construction observable, produces a more precise estimate which does not depend on the specific initial condition of the unobserved r^*.

Figure 8: Sensitivity to initial conditions: HLW and local level models

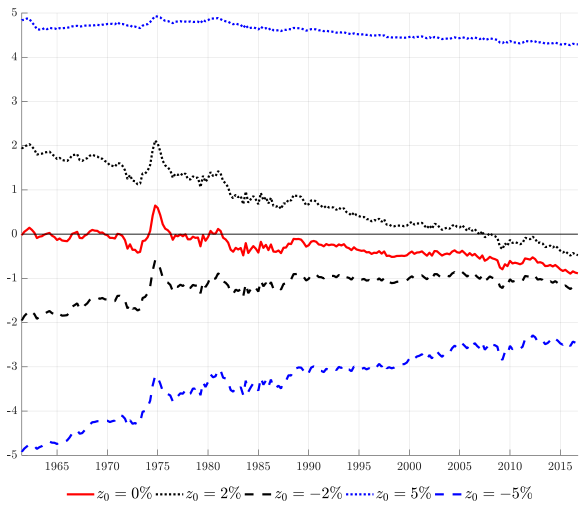

(a) z component, HLW model

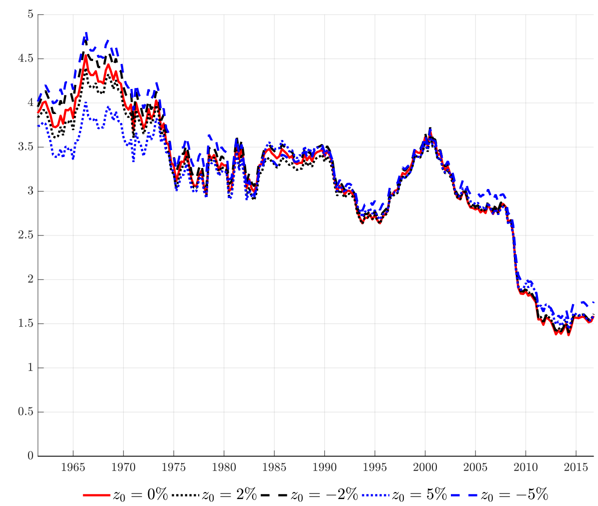

(b) Trend growth, HLW model

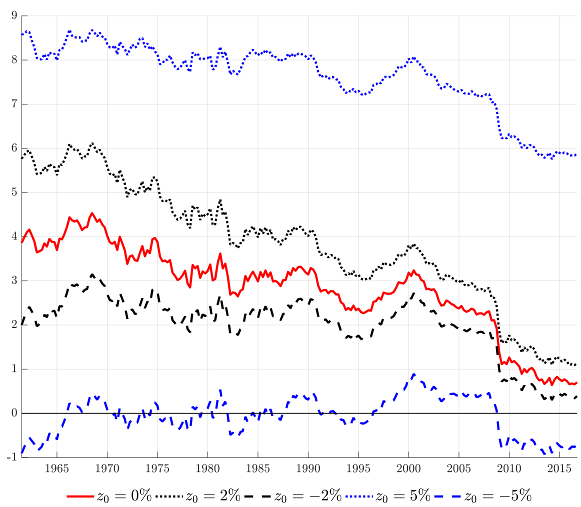

(c) r^*, HLW model

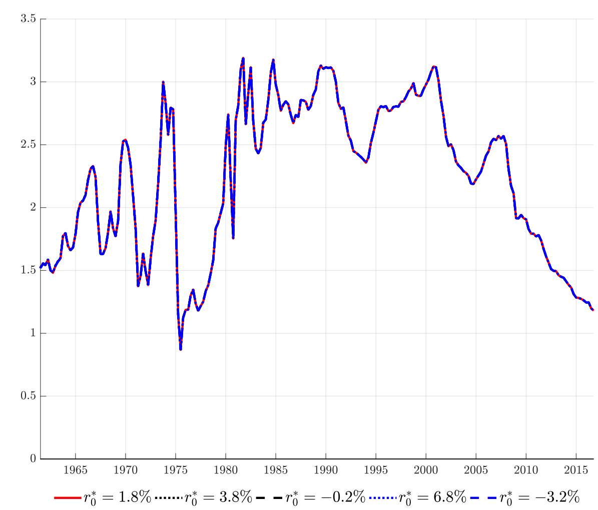

(d) r^*, Local level model

Notes: quarterly data, 1961Q2-2016Q3. Panels (a), (b), and (c) report the estimated z-component, annualized trend growth, and natural rate by the HLW model for different initial conditions z_0 of the z-component, with $z_0 \in \{-5, -2, 0, 2, 5\}$, and benchmark initial condition being $z_0 = 0$. Panel (d) reports the estimated natural rate by the local level model for different initial conditions r_0^*, with $r_0^* \in \{-3.2\%, -0.2\%, 1.8\%, 3.8\%, 6.8\%\}$ and benchmark initial condition being $r_0^* = 1.8$.

3.2 Historical International Evidence on r^*

We collect historical data at annual frequency over the period 1891-2016 for a set of seventeen advanced economies. Estimating the HLW model over such a sample inevitably produces flat IS and Phillips curves for two reasons: (i) the low frequency of the annual data is too coarse to identify any relation among output gap, interest rate gap, and inflation; and (*ii*) the long time span, which includes two World Wars, features several structural breaks in the relationships among those variables. Conversely the local level model, which does not rely on any specific structural relation, can be conveniently estimated in these circumstances so to shed light on the historical and international evidence on r^*.

Data on nominal short-term interest rates and CPI inflation rates come from the Jordà-Schularick-Taylor (2017) Macrohistory Database, which spans more than one century of data (1891-2013). We extend the sample until 2016 using data from the OECD Main Economic Indicators.[11] In order to compute the ex-ante real interest rate, we construct inflation expectations by estimating a sequence of first-order autoregressive models on realized inflation with rolling twenty-years windows, similarly to Hamilton et al. (2016). Cross-country distributions of nominal interest rates, inflation, and inflation expectations, are plotted in Figure 19 in the Appendix.

Figure 9 plots the cross-country distribution of real interest rates over the period 1891-2016. Real interest rates largely fluctuate over the sample, especially during the first and second World Wars, during which they become highly negative, as already emphasized by Hamilton et al. (2016) and Jordà et al. (2019). When focussing on the post-WW2 period, we observe a marked rise and fall of real interest rates, which starts around the 1960's, peaks about the end of the 1980's, and gradually falls until converging to very low or even negative levels in 2000's. Jordà et al. (2019) also document the rise and fall of the real safe rate, pointing out that, from a long-run perspective, the relevant question is why the safe rate was so high in the mid-1980's, rather than why it has declined so much since then.

We investigate further the rise and fall of the real interest rate by estimating the

[11] Specifically, we consider data for: Australia, Belgium, Canada, Denmark, Finland, France, Germany, Italy, Japan, Netherlands, Norway, Portugal, Spain, Sweden, Switzerland, United Kingdom and United States. Data feature missing values and outliers. We identify as outliers those observations for which the nominal short-term interest rate or the CPI inflation are in absolute value greater than 20%, and we treat those outliers as missing observations. We construct a balanced panel of data by filling missing values with values predicted by an estimated common factor model on observed real rates, which deals with missing observations through the approach described in Mariano and Murasawa (2003).

Figure 9: Real interest rates across countries

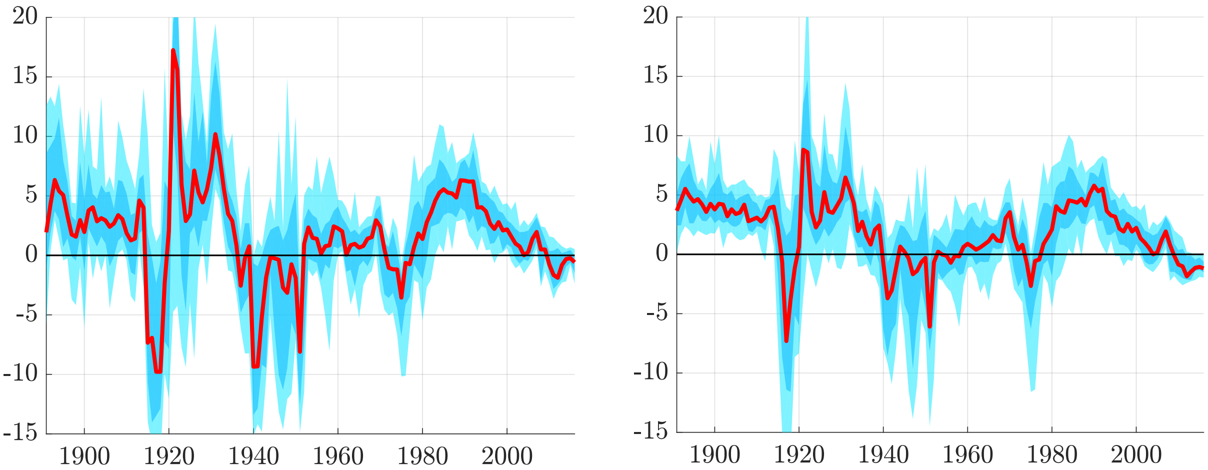

(a) Ex-post real rate

(b) Ex-ante real rate

Notes: annual data, 1891-2016. Cross-country median in red, 68% and 90% bands in dark and light blue, respectively. Data come from the Jordà-Schularick-Taylor (2017) Macrohistory Database and OECD Main Economic Indicators.

natural interest rate of each economy under study. Specifically, we fit a local level model for annual data on the ex-ante real interest rate for each country i as follows

$$r_{i,t} = r^*_{i,t} + \tilde{r}_{i,t}, \tag{15}$$

$$r^*_{i,t} = r^*_{i,t-1} + \varepsilon^{r^*}_{i,t}, \tag{16}$$

where the innovation to the natural interest rate, $\varepsilon^{r^*}_{i,t}$, is serially uncorrelated with variance $\sigma^2_{r^*_i}$. To reduce the influence of extreme observations, especially during the first and second World Wars, we allow the variance of the interest rate gap to vary over time according to an ARCH(1) process, as in Hamilton et al. (2016). Specifically,

$$\begin{aligned} \tilde{r}_{i,t} &= h^{1/2}_{i,t} e_{i,t} \qquad e_{i,t} \sim N(0,1) \\ h_{i,t} &= \delta_{i,0} + \delta_{i,1} \tilde{r}^2_{i,t-1} \end{aligned}$$

Even though the presence of ARCH effects makes the system conditionally non-Gaussian, we are still able to carry out the estimation via the Kalman filter using the approximation in Harvey et al. (1992). We initialize the filter by setting $r^*_{i,1|1} = r_{i,1}$, with a diffuse prior for the variance of the initial observation. To help convergence, we impose nonnegativity constraints on $\sigma^2_{r^*,i}$ and $\delta_{i,0}$, and we restrict $\delta_{i,0}$ to be between 0 and 1. Finally, we compute

Figure 10: Estimated natural rates across countries: 1891-2016

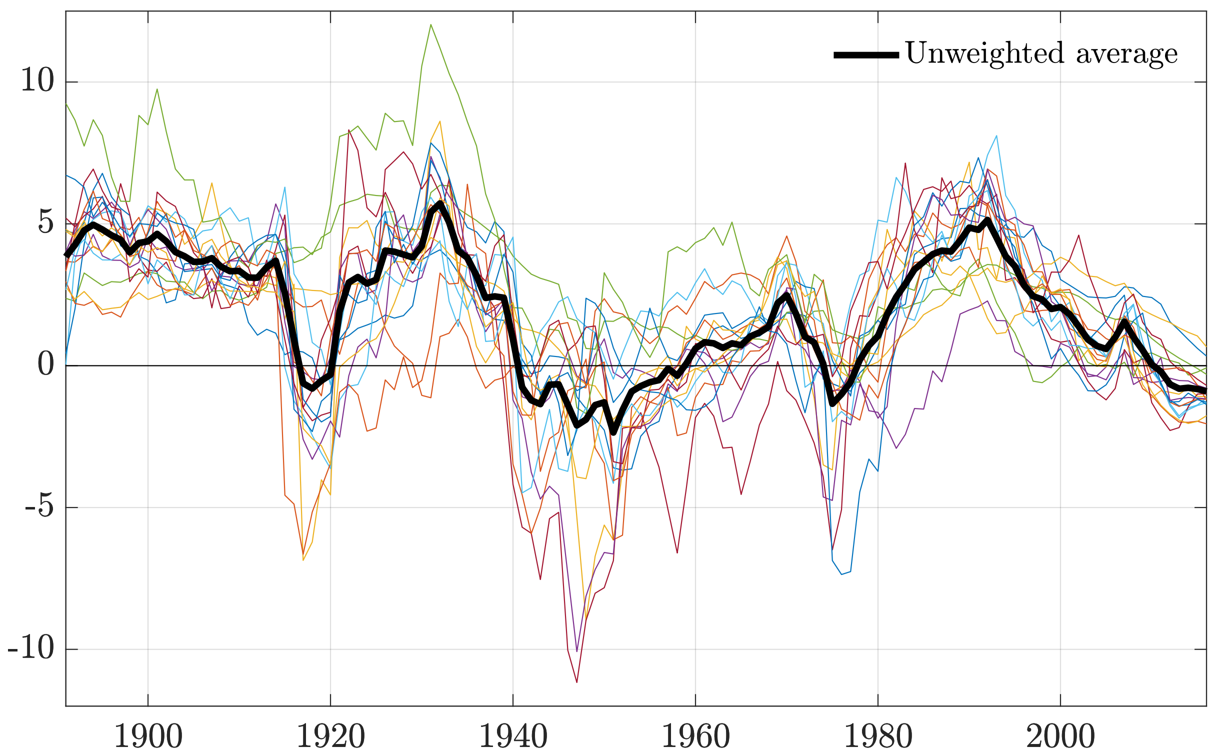

Notes: annual data, 1891-2016. Estimated r^* across countries. Black solid line refers to the unweighed average.

confidence bands of the one-sided filtered natural rate by applying Hamilton's (1986) approach, which deals with both filter and parameter uncertainty, with 2000 replications of the parameter vector. Figure 21 in the Appendix plots the estimated country-specific volatilities of the interest rate gap, confirming that ARCH effects adequately capture the large fluctuations associated with the two World Wars.

Figure 10 plots the estimated r^* for all countries in the sample, together with their unweighed average (black solid line). We observe a strong comovement in the estimated natural interest rates. Most of the rates closely follow the average, especially so after the 1960's, thereby suggesting a strong international synchronization of interest rates. We document a general decline in natural interest rates which starts from the beginning of the twentieth century until roughly the 1960's. Thereafter, natural interest rates follow a generalized rise and fall which peaks around the end of the 1980's. Eventually, rates converge to very low, or even negative levels over the 2000's. While most of the literature

Figure 11: Estimated natural rates: U.S. and euro area

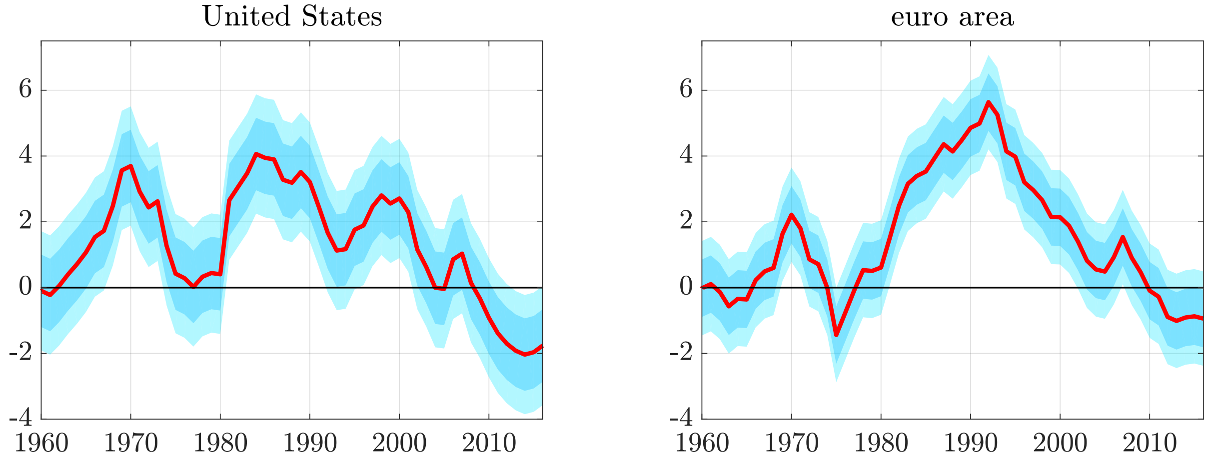

Notes: annual data, 1960-2016. Estimated r^* jointly with the 68% and 90% bands. Bands, which reflect both filter and parameter uncertainty, are computed using Hamilton's (1986) approach with 2000 replications.

has already emphasized the gradual fall of the natural interest rate that occurred since the early 1990's, here we put the dynamics of the rate in a long-run perspective and focus on the rise and fall which occurred over the post-WW2 period.

This rise and fall in the natural interest rate appears to be statistically significant for most of the countries. Figure 20 in the Appendix reports the estimated natural rates and the associated 90% bands for each country. We also construct a measure of the natural interest rate for the euro area by aggregating individual rates of Eurozone member countries using GDP-based weights over the period 2000-2016. Figure 11 compares the natural interest rate of the United States with the one of the euro area by plotting both estimates with 68% and 90% bands. As can be seen, the rise and fall pattern is significant in both currency areas, with a peak around the mid-1980's for the United States, and in the early 1990's for the euro area.

3.3 What has Driven the Rise and Fall in r^*?

The next question that we pose is: what has driven the rise and fall of the natural interest rate? The local level model does not speak about the drivers of r^* because it exploits data on the interest rate only. Still, we can exploit the cross-country variation on the estimated natural rates to draw important insights about some characteristics of

Figure 12: The rise and fall of the natural interest rate

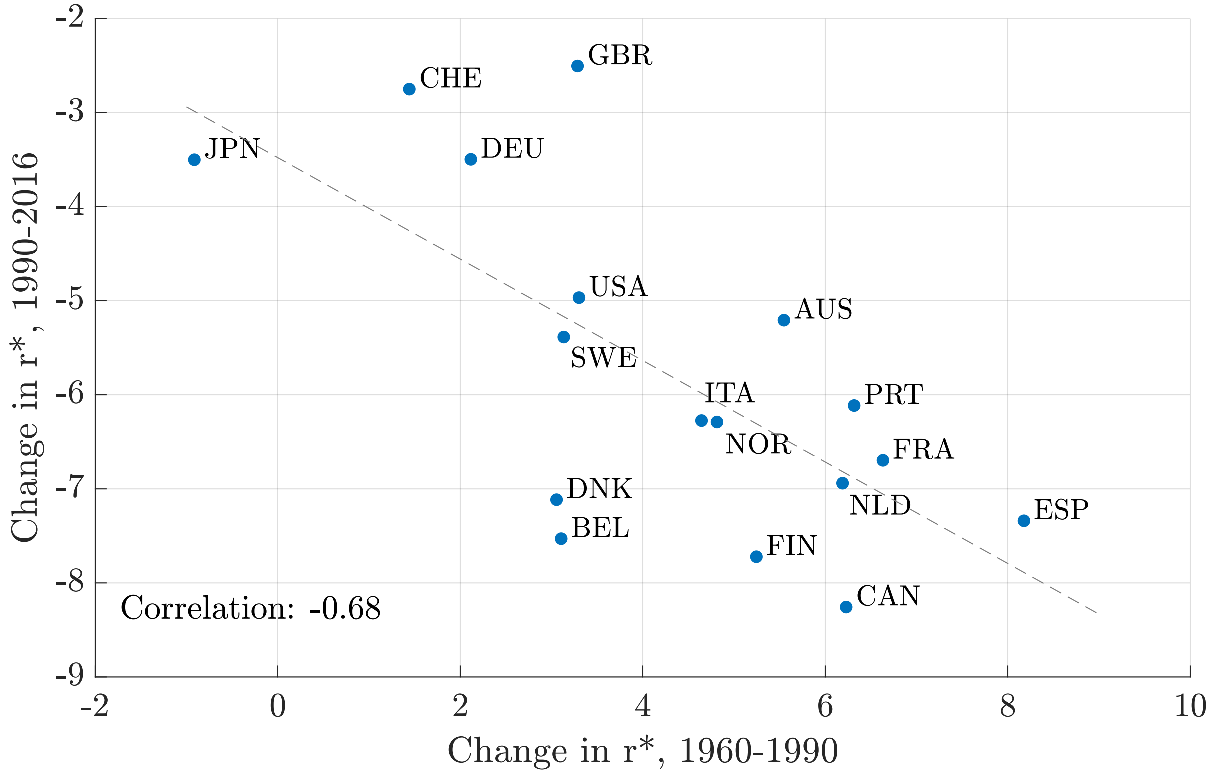

Notes: the chart reports in the x-axis, the change in the natural interest rate between 1960 and 1990, in the y-axis, the change in the natural interest rate between 1990 and 2016.

the underlying drivers of the rise and fall that we have documented.

Figure 12 plots the change in the estimated natural rate between 1960 and 1990 against the corresponding change between 1990 and 2016. We highlight two results. First, there is a large synchronization of natural rates, as most of them increase over the 1960-1990 period (with the interesting exception of Japan), and generally fall afterwards. This evidence suggests the presence of common, or *global*, factors, which may have played an important role in driving the variation of natural rates across countries. And second, countries which feature larger falls in the natural rate since the 1990's are also those for which the rate increased faster since the 1960's. The relationship appears to be strong, with an average correlation of -68%. This evidence confirms that both the rise and fall in the natural interest rate may be the result of the same factor. Hence, any hypothesis that seeks to explain the fall in interest rates should also be consistent with explaining the precedent rise.

To shed further light on the factors behind the rise and fall, we estimate the following Panel Error Correction Model (ECM)

$$\Delta r_{i,t} = \alpha \left(r_{i,t-1} - \beta' X_{i,t-1} \right) + \gamma' \Delta X_{i,t} + \varepsilon_{i,t}, \tag{17}$$

where each country is denoted by i, $r_{i,t}$ is the observed real interest rate, and $X_{i,t}$ is a vector of indicators of potential drivers of the natural interest rate. The rationale behind equation (17) is the following: if there exists a long-run cointegration relationship between a number of unobserved factors and the natural interest rate, then there must exist cointegration between the measures of those factors and the observed real interest rate. Moreover, the regression model (17) yields an alternative measure for the natural interest rate, which is given by the estimated linear combination of the observed factors, $\hat{\beta}' X_{i,t}$. This measure can then be decomposed further in terms of the contributions of each factor. We provide further details in the Appendix.

We collect cross-country data on potential drivers of the natural interest rate over the period 1960-2016 by relying on the existing theoretical literature. We identify three factors which can be plausibly considered exogenous determinants: (*i*) productivity growth; (*ii*) demographic composition; and (*iii*) risk. We acknowledge that we deal with a narrow set of potential factors, but this limitation is attributable to two reasons. First, the lack of available historical cross-country data is a serious constraint for our analysis. And second, we refrain from considering those drivers which are likely to be endogenous to the natural interest rate or to some other specific factors which we are already including in the analysis. Our exercise should then be interpreted as confronting three different hypotheses to the data, given the caveat that we are not considering the entire set of potential explanations behind the evolution of the natural interest rate.[12]

Changes in productivity, by affecting the propensity to invest, may play an important role in determining the natural interest rate. This explanation follows the traditional

[12] Another important caveat is that, while the literature has traditionally considered productivity, demographics, and risk as independent, recent papers emphasize the potential connections among them. See for instance Aksoy et al. (2019), which propose a theoretical model in which demographic changes, by affecting the rate of innovation, may shape the evolution of productivity.

Figure 13: Cross-country data for the Panel ECM estimation

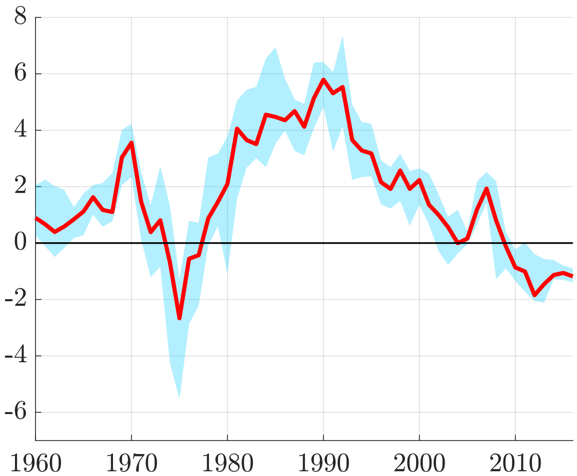

(a) Real ex-ante rate

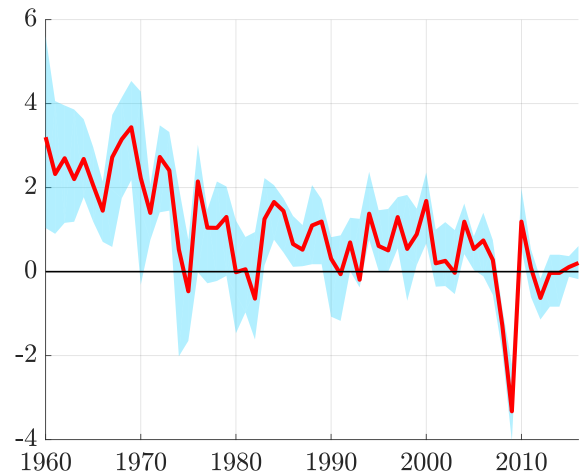

(b) TFP growth

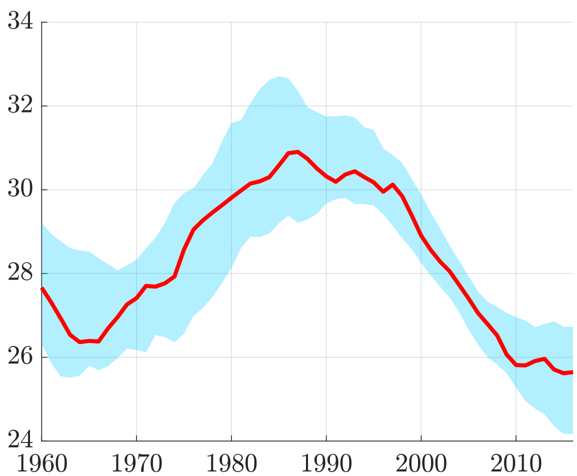

(c) Young-age population share

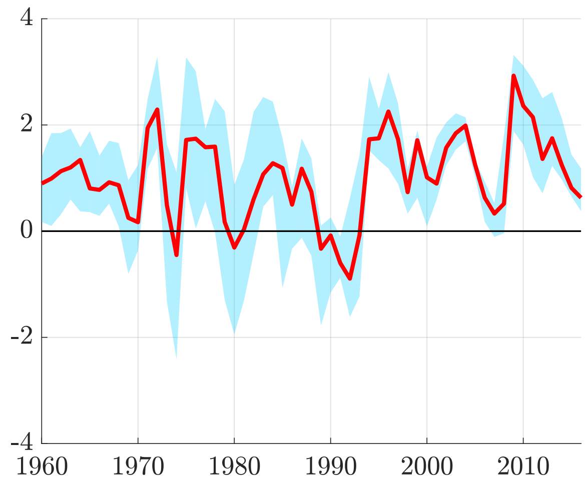

(d) Term spread

Notes: annual data, 1960-2016, for 17 economies. Cross-country median (in red) and interquartile range (in blue). Data on TFP come from Penn World Tables, Total Economy Database. Young-age population share (20-39 years old) come from the Human Mortality Database. Term spread is defined as the long-term minus short-term rates, where data come from the Jordà-Schularick-Taylor (2017) Macrohistory Database and OECD Main Economic Indicators.

logic of the basic New Keynesian model, according to which the only source of variation in the natural interest rate is the growth of productivity. In this respect, Gordon (2012, 2014) suggests that the United States and various advanced economies are experiencing a productivity slowdown due to a decline in the innovation rate. Following this logic, the productivity slowdown may be responsible for the current low levels of the natural interest rate. HLW2017 provide evidence to support this hypothesis by showing that the synchronized fall in the natural interest rate in the United States and other advanced economies may be attributable to a generalized slowdown of trend growth. We collect cross-country data on TFP growth from the Penn World Tables, extended forward to the year 2016 with data from the Total Economy Database. Figure 13 plots the cross-country distribution of TFP growth. As can be seen, productivity growth is very volatile and steadily declines over time, reflecting the aforementioned productivity slowdown phenomenon.

Changes in the demographic composition may also have an important effect on the natural interest rate, for instance by affecting the aggregate propensity to save of the economy. Most of the literature has emphasized the gradual process of population ageing as having a plausible downward effect on the natural rate. Ageing induces people to accumulate savings during their working lives so as to be able to pay for their retirement. In this paper, we also emphasize that the United States and many other advanced economies experienced a dramatic baby boom after the Second World War, which temporarily raised the share of young workers in the population. To the extent that the young workers supply labor and have relatively low savings rate, as documented for instance in Higgins (1998), the baby boom might have led to a temporary rise of the natural interest rate. For that reason, we obtain cross-country data on demographic composition from the Human Mortality Database, a joint project developed by the University of California and the Max Planck Institute for Demographic Research. We construct a measure of young-age population share, calculated as the ratio of the population aged between 20 and 39 over total population. Figure 13 plots the cross-country distribution of this share. The series is markedly smooth and features large comovements. We observe the effects of the baby boom in many advanced economies: a temporary increase since the 1960's, with a peak around the end of the 1980's. Once the baby boom ends, the share gets back to its negatively sloped trend, presumably driven by the process of population ageing.

The final determinant that we consider is based on the idea that higher risk may drive down the natural rate by increasing the propensity of the households to save. In this respect, Gerali and Neri (2018) estimate a DSGE model for the United States and the euro area which shows that risk premium shocks, capturing precautionary savings motives due to heightened uncertainty, have driven down the natural interest rate in both currency areas. Related to this logic, Del Negro et al. (2017) emphasize the role of spreads between Treasury and corporate bonds, finding that safety and liquidity premia have reduced the U.S. natural interest rate since the 1990's. Further, Caballero and Farhi (2017) also show how episodes of scarcity of safe assets can reduce the natural interest rate. We collect data on the spread between long-term and short-term interest rates as an imperfect proxy for the term premium to measure the time-varying risk aversion of the agents. Once again, data until 2013 come from the Jordà-Schularick-Taylor (2017) Macrohistory Database, but we extend the sample until 2016 using data from the OECD Main Economic Indicators database. Figure 13 plots the cross-country distribution of the term spread. As can be seen, the spread is very volatile, it starts to increase in the 1990's and peaks during the Great Recession.

We estimate the Panel ECM of (17) in which the dependent variable is the real ex-ante interest rate. We add either a common intercept or a country-specific constant to allow for some heterogeneity across countries. Table 1 reports the results of those regressions. In both specifications, the loading coefficient is not only statistically significant but also lies between -1 and 0, which is evidence of cointegration among the variables. We find a weak link of TFP growth with the real interest rate: the associated coefficient is not statistically significant in either version of the regression. This finding complements recent results in Lunsford and West (2019), who find a negative rather than positive long-run correlation between the safe rate and TFP growth for the United States. This result is also in line with Hamilton et al. (2016), who find a tenuous relationship between average real rates and trend GDP growth using historical data for a large set of OECD economies. On the other hand, risk is negatively related to the real interest rate, and the relationship is statistically significant in either version of the regression. This result is in line with

Table 1: Panel ECM estimation results

Loading	-0.22***	-0.25***
	(0.02)	(0.02)
TFP growth	0.18	0.14
	(0.14)	(0.12)
Risk	-0.73***	-0.77***
	(0.15)	(0.14)
Young share	0.41***	0.49***
	(0.09)	(0.09)
Intercept	Common	Country-specific

Note: The dependent variable is the real ex-ante interest rate, measured in percentages at annual rate. TFP growth is measured in percentages. Risk is the spread between long- and short-term interest rates, both measured in percentages at annual rate. Young share is the share of people aged 20-39 years old over total population, measured in percentages. Balanced panel for 17 countries at annual frequency (1960-2016). Standard errors in parentheses. *, **, *** respectively denote significance at the 10%, 5%, and 1%.

the mechanism emphasized in Gerali and Neri (2018), according to which heightened risk increases the precautionary savings motive of the agents, thereby decreasing the natural interest rate.

Finally, we observe that the young-age population share is positively related to the real interest rate. This result is consistent with the recent literature emphasizing population ageing as responsible for the current low levels of real interest rates. Again, this result is also in line with Lunsford and West (2019), who find a negative long-run correlation of the U.S. real interest rate with the share of 40- to 64-year-old in the population.

Figure 14: Estimated r^* by Panel ECM and local level model: selected economies

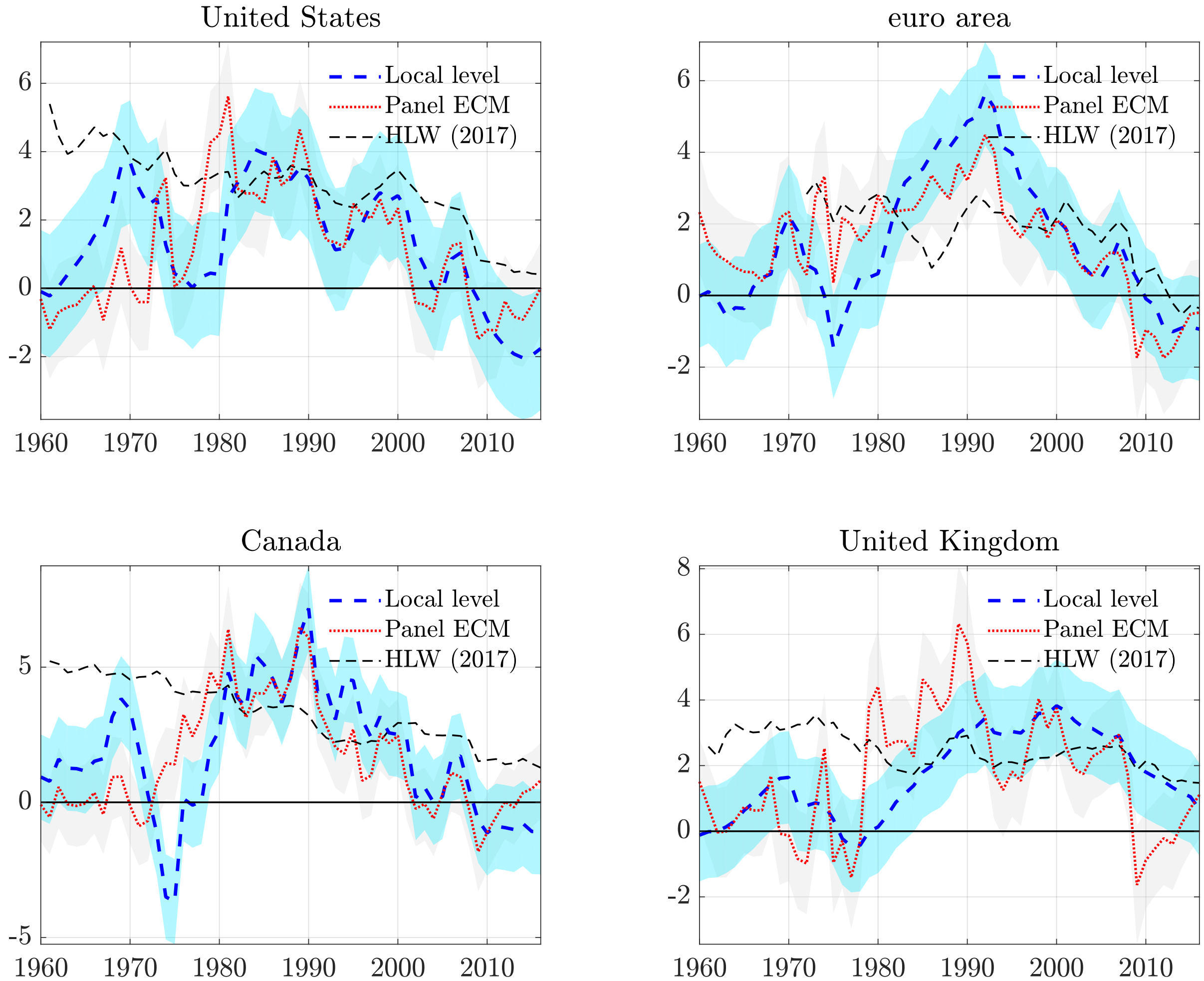

Notes: annual data, 1960-2016, for 17 economies. Local level model estimates in dashed blue jointly with 90% confidence bands, Panel ECM estimates in dotted red jointly with 90% confidence bands. Results from HLW (2017) in dashed black for the United States, Canada, and United Kingdom over the period 1961-2016, for the euro area over the period 1972-2016.

Figure 14 plots the estimated natural interest rates by the Panel ECM and the local level model and the corresponding 90% confidence bands for the US, euro area, Canada, and UK. We also report results of HLW (2017) for the same economies, whose results at quarterly frequency over the period 1961Q1-2016Q4 (1972Q1-2016Q4 for the euro area) have been averaged at the yearly frequency. The Panel ECM results predict a statistically significant rise and fall of the natural interest rate over the sample, which closely follow findings of the local level model. The same result holds for many other countries in the sample, as reported in Figure 22 in the Appendix. Thus, our results largely confirm the findings in HLW (2017) about the fall of the natural interest rate since the 1990's. Nevertheless, we emphasize a discrepancy in the behavior of r^* prior that date: while HLW (2017) predicts a steady decline of the natural rate over the entire sample, largely due to a slowdown in trend growth, our two alternative but complementary approaches predict a rise of the natural interest rate until approximately the end of the 1980's. Therefore, one relevant question we may ask is why the natural interest rate was so high over the 1980's-1990's, as well as why it has declined so much since then.

Figure 15: What explains the rise and fall?

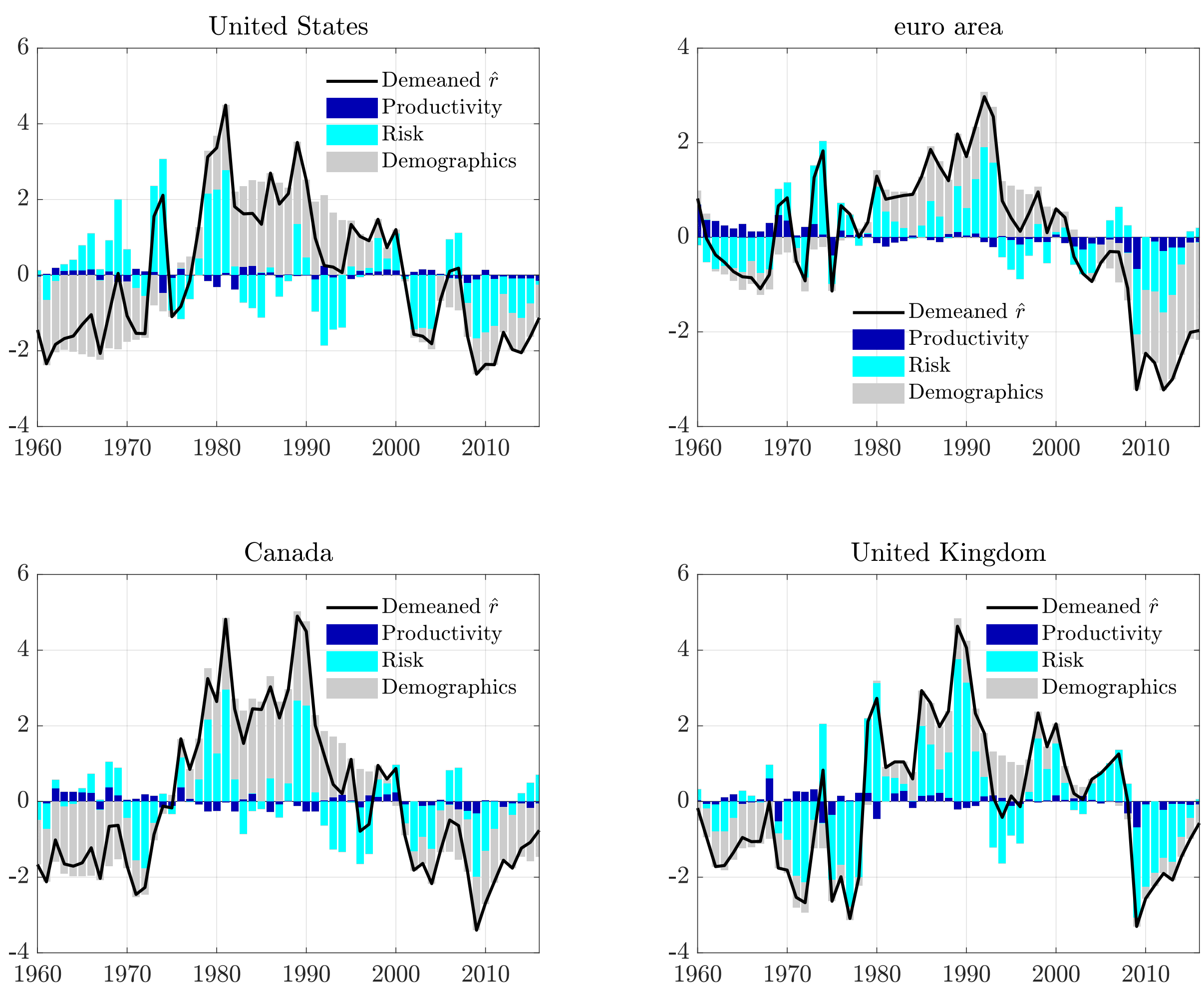

Notes: annual data, 1960-2016. Solid black line refers to the estimated (demeaned) natural interest rate estimated by the Panel ECM. Bars correspond to the individual contributions of productivity growth, risk, and demographic composition.

We tackle the question on what has driven the rise and fall of r^* by computing the contributions of each factor to the real interest rate predicted by the Panel ECM model.

Figure 15 plots the estimated natural interest rates for the US, euro area, Canada, and UK, demeaned so to abstract from the contribution of the intercept, together with each driver's contribution. In general, we observe a minor role for productivity growth in most countries. Risk explains part of the rise of the real interest rate, and a substantial component of the fall since roughly the 1990's. Demographic composition plays a key role in affecting the natural interest rate, particularly so for the U.S. and Canada. Since the 1960's, the young-age population rises due to the dramatic baby boom experienced in those economies, which coincides with a steady increase in the real rate. Once the baby boom ends, the share of young in the population falls, and simultaneously real interest rates gradually fall too.

To isolate the role of demographics, Figure 16 compares the estimated natural interest rate with the version that abstracts from productivity growth and risk, for a select group of countries. As can be seen, changes in demographic composition account for most of the rise and fall of the natural interest rate in US, the euro area, and Canada. Interestingly, demographics account for the dynamics of r^* in Japan too, which experienced the demographic transition much earlier than the rest of advanced economies, consistently predicting the absence of the rise and fall of the natural interest rate for this economy.

Figure 16: The role of demographics

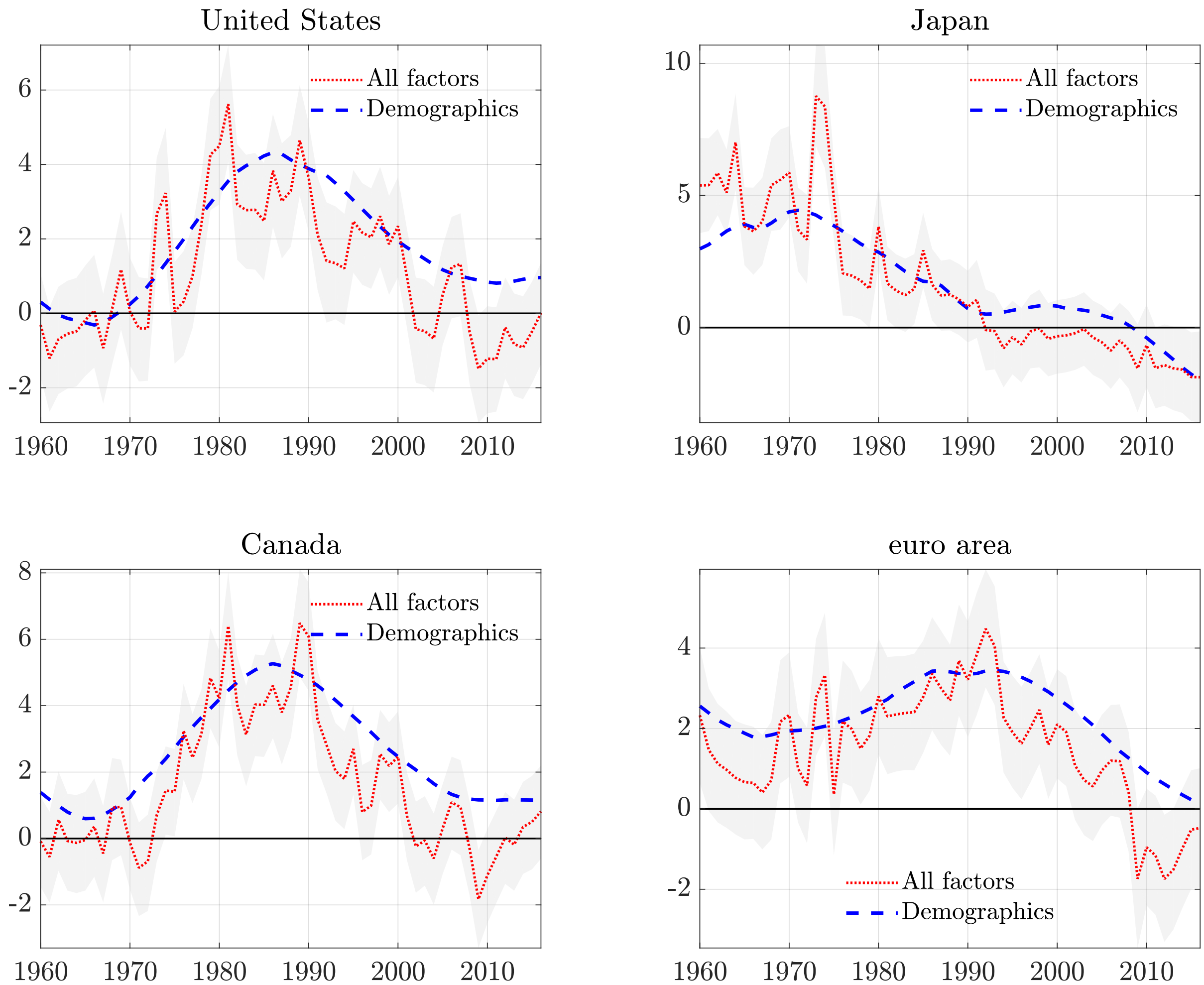

Notes: annual data, 1960-2016. Panel ECM estimated natural interest rate in dotted red jointly with 90% confidence bands; estimated natural interest rate which abstracts from productivity growth and risk in dashed blue.

To provide an overall assessment of factors shaping the rise and fall across countries, Figure 17 reports for each country the changes in the estimated natural interest rate over the periods 1960-1990 and 1990-2016, as well as the contributing factors. The evolving demographic composition appears to have played a key role in shaping developments of r^*, especially so for the post-1990's fall. Risk factors have also played a non-negligible role, particularly in the United Kingdom and Portugal. Finally, our results confirm a minor role for productivity growth in explaining the rise and fall of r^*.

Figure 17: Changes in r^* and contributions: the rise (1960-1990) and fall (1990-2016)

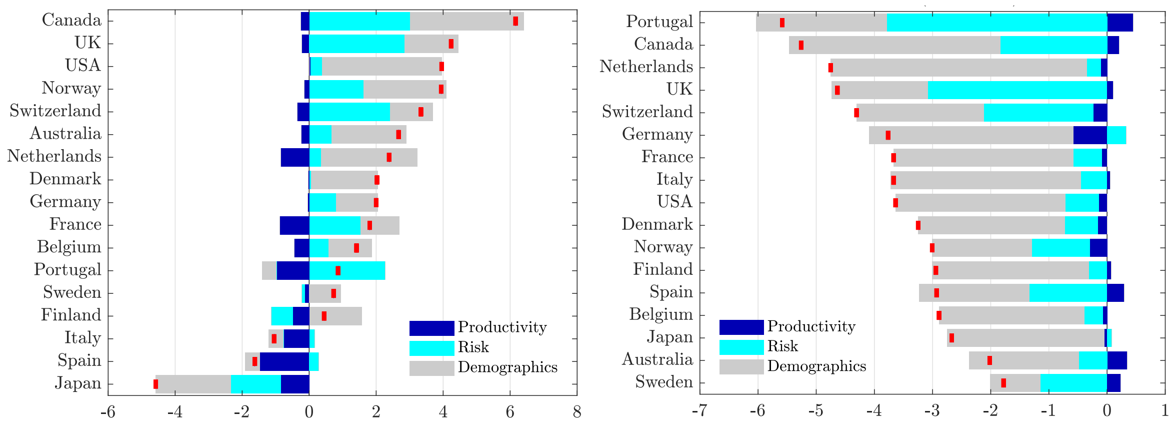

(a) Change 1960-1990

(b) Change 1990-2016

Notes: Red dots denote changes in estimated r^* over the period 1960-1990 (panel a) and over the period 1990-2016 (panel b), in percent. Bars correspond to the individual contributions of productivity growth, risk, and demographic composition.

4 Conclusions

In this paper we shed some light on the fundamental source of uncertainty that plagues the workhorse model of LW2003, which tries to measure the natural interest rate. We show that the model is generally able to produce very accurate estimates of r^*. However, the precision of the model dramatically drops when either the output gap is insensitive to the real interest rate gap (flat IS curve), or if inflation is insensitive to the output gap (flat Phillips curve). In those cases, the model fails the observability condition, which ensures that the unobserved states can be uniquely determined by the data. Unfortunately, those cases are empirically relevant according to the estimates in the literature.

Nevertheless, we show that after imposing stationarity of the interest rate gap, the LW2003 model can identify both the growth and non-growth components of r^* even when the IS and Phillips curves are flat. The extra identification restriction comes from the fact that the observed real rate can be decomposed into a transitory component (interest rate gap) and a permanent component (the natural rate). A direct implication of this finding is that, if a researcher is interested in estimating r^* but not necessarily its components, then a valid alternative is to estimate a univariate local level model which decomposes the observed real interest rate into its permanent and transitory components. The permanent component closes the interest rate gap, and consistently stabilizes both the output gap and inflation under a general class of New Keynesian models.

Obviously, the local level model cannot identify the growth and non-growth components of r^*, because it exploits data on the interest rate only. However, it is robust to situations in which either the estimated IS or the Phillips curves are flat, because the model is always observable.

We employ historical data at the annual frequency for a set of seventeen advanced economies over the period 1891-2016 to test the validity of the local level model. We find a common decline of r^* across most countries since the start of the twentieth century until the 1960's. Subsequently, a marked rise and fall occurs, peaking around the end of the 1980's. Interestingly, countries which feature larger falls in the natural rate since the 1990's are also those for which the rate increased more over the period 1960's – 1980's. This evidence suggests that both the rise and fall of r^* may be the result of common drivers, and that any hypothesis that seeks to explain the fall in interest rates should be able to explain the precedent rise too.

Since the local level model is silent about the drivers of the estimated r^*, we investigate the rise and fall of r^* by estimating a Panel ECM using data on the observed real interest rate and a set of indicators for productivity growth, demographic composition and risk. Through the lens of the model, we find that demographics can account for the bulk of the rise and fall in the natural interest rate. Specifically, the observed rise can be explained by a temporary rise in the proportion of young workers due to the dramatic baby boom experienced in most economies. Once the baby boom ends, the share of young workers gets back to its previous negatively trended path, due to the process of population ageing. This evidence supports recent studies which emphasize the crucial role of demographics for the evolution of safe real rates. An important caveat, though, is that data availability and endogeneity concerns limit our analysis to a narrow set of potential underlying factors. Therefore, our results should be interpreted as providing suggestive evidence that the evolving demographics may be the key to understand the generalized rise and fall in r^*. We leave for further research the possibility of a horse-race against a more comprehensive set of hypotheses.

References

Aksoy, Y., H. S. Basso, R. Smith, and T. Grasl (2019) "Demographic Structure and Macroeconomic Trends". *American Economic Journal: Macroeconomics* 11, 193-222.

Andrews, D., and W. Ploberger (1994) "Optimal tests when a nuisance parameter is present only under the alternative". *Econometrica* 62, 1383-1414.

Beyer, R. C. M., and V. Wieland (2019) "Instability, imprecision, and inconsistent use of equilibrium real interest rate estimates". *Journal of International Money and Finance* 94, 1-14.

Barsky, R., A. Justiniano, and L. Melosi (2014) "The natural rate of interest and its usefulness for monetary policy". *American Economic Review* 104, 37-43.

Berger, T. and B. Kempa (2014) "Time-varying equilibrium rates in small open economies: Evidence for Canada". *Journal of Macroeconomics* 39, 203-214.

Brand, C., M. Bielecki, and A. Penalver (2018) "The natural rate of interest: estimates, drivers, and challenges to monetary policy ". *ECB Occasional Paper* 217.

Caballero, R. J., and E. Farhi (2017) "The safety trap". *The Review of Economic Studies* 85, 223-274.

Carvalho, C., A. Ferrero, and F. Nechio (2016) "Demographics and real interest rates: Inspecting the mechanism". *European Economic Review* 88, 208-226.

Christensen, J. H. E., and G. D. Rudebush (2017) "A New Normal for Interest Rates? Evidence from Inflation-Indexed Debt". *Review of Economics and Statistics*, 1-46.

Clark, T.E., and S. Kozicki (2005) "Estimating equilibrium real interest rates in real time". *The North American Journal of Economics and Finance* 16, 395-413.

Cour-Thimann, P., R. Pilegaard, and L. Stracca (2006) "The output gap and the real interest rate gap in the euro area, 1960-2003". *Journal of Policy Modeling* 28, 775-790.

Crespo Cuaresma, J., E. Gnan, and D. Ritzberger-Gruenwald (2004) "Searching for the Natural Rate of Interest: A Euro Area Perspective". *Empirica* 31, 185-204.

Cúrdia, V., A., Ferrero, G. C. Ng, and A. Tambalotti (2015) "Has US monetary policy tracked the efficient interest rate?". *Journal of Monetary Economics* 70, 72-83.

Del Negro, M., D., Giannone, M. P. Giannoni, and A. Tambalotti (2017) "Safety, liquidity, and the natural rate of interest". *Brookings Papers on Economic Activity* No. 1, 235-316.

Favero, C. A., and V. Galasso (2016a) "Demographics and the Secular Stagnation". In: *After the Crisis: Reform, Recovery, and Growth in Europe.* Edited by F. Caselli, M. Centeno, and J. Tavares. Oxford University Press.

Favero, C. A., Gozluklu, A. E., and H. Yang (2016b) "Demographics and the behavior of interest rates". *IMF Economic Review* 64, 732-776.

Ferrero G., M. Gross, and S. Neri (2019) "On secular stagnation and low interest rates: demography matters". *International Finance*, forthcoming.

Gagnon, E., B. K. Johannsen, and J. D. Lopez-Salido (2016) "Understanding the New Normal: the role of demographics". *FEDS Working Paper* No. 2016-080.

Galí, J. (2008) *Monetary Policy, Inflation, and the Business Cycle. An Introduction to the New Keynesian Framework.* Princeton University Press.

Garnier, J., and B-R. Wilhelmsen (2009) "The natural rate of interest and the output gap in the euro area: a joint estimation". *Empirical Economics* 36, 297-319.

Gerali, A., and S. Neri (2018) "Natural rates across the Atlantic". *Journal of Macroeconomics*, in press.

Giammarioli, N., and N. Valla (2003) "The natural real rate of interest in the euro area". *European Central Bank Working Paper Series* No. 233.

Gordon, R. J. (2012) "Is US economic growth over? Faltering innovation confronts the six headwinds". *National Bureau of Economic Reasearch Working Paper* No. 18315.

Gordon, R. J. (2014) "The demise of US economic growth: Restatement, rebuttal, and reflections". *National Bureau of Economic Reasearch Working Paper* No. 19895.

Hamilton, J. D. (1986) "A standard error for the estimated state vector of a state-space model". *Journal of Econometrics*, 333, 387-397.

Hamilton, J. D., E. S. Harris, J. Hatzius, and K. D. West (2016) "The equilibrium real funds rate: Past, present, and future". *IMF Economic Review*, 64, 660-707.

Harvey, A. (1989) *Forecasting, structural time series models and the Kalman filter*. Cambridge University Press.

Harvey, A., E. Ruiz, and E. Sentana (1992) "Unobserved component time series models with ARCH disturbances". *Journal of Econometrics*, 52, 129-157.

Higgins, M. (1998) "Demography, national savings, and international capital flows". *International Economic Review*, 343-369.

Holston, K., T. Laubach, and J. C. Williams (2017) "Measuring the natural rate of interest: International trends and determinants". *Journal of International Economics* 108, S59-S75.

Human Mortality Database. University of California, Berkeley (USA), and Max Planck Institute for Demographic Research (Germany). Available at www.mortality.org or www.humanmortality.de.

Jordà, O., M. Schularick, and A. M. Taylor (2017) "Macrofinancial history and the new business cycle facts". *NBER Macroeconomics Annual*, 31, 213-263.

Jordà, O., K. Knoll, D. Kuvshinov, M. Schularick, and A. M. Taylor (2019) "The Rate of Return on Everything, 1870-2015". *The Quarterly Journal of Economics*, 134, 1225-1298.

Juselius, M., C. Borio, P. Disyatat, and M. Drehmann (2017) "Monetary Policy, the Financial Cycle, and Ultra-Low Interest Rates". *International Journal of Central Banking*, 13, 55-89.

Kalman, R. E. (1960) "On the general theory of control systems". Proc. First Interntational Congress on Automatic Control, Moscow.

Kiley, M. (2015) "What can the data tell us about the equilibrium real interest rate?". *Finance and Economics Discussion Series*, 2015-077. Board of Governors of the Federal Reserve System.

Kuhn, L., F. Ruch, and R. Steinbach (2017) "Reaching for the (r)-stars: estimating South Africa's neutral real interest rate". *SARB Working Papers*.

Kuttner, K. N. (1994) "Estimating potential output as a latent variable". *Journal of Business & Economic Statistics*, 12, 361-368.

Laubach, T. (2001) "Measuring the NAIRU: evidence from seven economies". *Review of Economics and Statistics*, 83, 218-231.

Laubach, T., and J. C. Williams (2003) "Measuring the Natural Rate of Interest". *Review of Economics and Statistics*, 85, 1063-1070.

Levin, A. T., and J. C. Williams (2003) "Robust monetary policy with competing reference models". *Journal of Monetary Economics*, 50, 945-975.

Lewis, K. F., and F. Vazquez-Grande (2019) "Measuring the natural rate of interest: A note on transitory shocks". *Journal of Applied Econometrics*, 34, 425-436.

Lisack, N., R. Sajedi, and G. Thwaites (2017) "Demographic trends and the real interest rate". *Bank of England Working Paper Series*, No. 701.

Lubik, T. A., and C. Matthes (2015) "Calculating the natural rate of interest: A comparison of two alternative approaches". *Richmond Fed Economic Brief*, October, 1-6.

Lunsford, K. G., and K. West (2019) "Some Evidence on Secular Drivers of US Safe Real Rates". *American Economic Journal: Macroeconomics*, forthcoming.

Mariano, R. S., and Y. Murasawa (2003) "A new coincident index of business cycles based on monthly and quarterly series". *Journal of Applied Econometrics*, 18, 427-443.

Mésonnier, J-S., and J-P. Renne (2007) "A time-varying "natural" rate of interest for the euro area". *European Economic Review*, 51, 1768-1784.

Neiss, K. S, and E. Nelson (2003) "The real-interest-rate gap as an inflation indicator". *Macroeconomic Dynamics*, 7, 239-262.

Orphanides, A., and J. C. Williams (2007) "Robust monetary policy with imperfect knowledge". *Journal of Monetary Economics*, 54, 1406-1435.

Pedersen, J. (2015) "The Danish natural real rate of interest and secular stagnation". *Danmarks Nationalbank Working Papers*, No. 94.

Pescatori, A. and J. Turunen (2015) "Lower for Longer: Neutral Rates in the United States". *International Monetary Fund Working Paper Series*, No. 135.

Rachel, L. and T. D. Smith (2017) "Are Low Real Interest Rates Here to Stay?". *International Journal of Central Banking*, 13, 1-42.

Stock, J. H. (1994) "Unit roots, structural breaks, and trends". In: R., Engle (Ed.), Handbook of Econometrics. Vol. 4. Elsevier Science, 2739-2841.

Stock, J. H., and M. W. Watson (1998) "Median unbiased estimation of coefficient variance in a time-varying parameter model". *Journal of the American Statistical Association*, 93, 349-358.

Taylor, J. B., and V. Wieland (2016) "Finding the equilibrium real interest rate in a fog of policy deviations". *Business Economics*, 51, 147-154.

Trehan, B. and T. Wu (2007) "Time-varying equilibrium real rates and monetary policy analysis". *Journal of Economic Dynamics and Control*, 31, 1584-1609.

Watson, M. W. (1986) "Univariate Detrending with Stochastic Trends". *Journal of Monetary Economics*, 18, 49-75.

Weber, A. A., W. Lemke, and A. Worms (2008) "How useful is the concept of the natural real rate of interest for monetary policy?". *Cambridge Journal of Economics*, 32, 49-63.

Woodford, M. (2003) *Interest and Prices.* Princeton University Press. 18, 49-75.

Wynne, M. A., and R. Zhang (2017) "Estimating the Natural Rate of Interest in an Open Economy". *Empirical Economics*, 1-28.

Wynne, M. A., and R. Zhang (2018) "Measuring the World Natural Rate of Interest". *Economic Inquiry*, 56, 530-544.

A Estimating the Holston, Laubach, & Williams Model

The estimation of the HLW model proceeds in three steps.

Step 1: First, by omitting the interest rate gap from equation (1) and by assuming that the trend growth rate is constant, we estimate a simpler model to recover a measure of potential output. Specifically, the state-space representation of the model reads

$$
\begin{aligned}
\begin{pmatrix} y_t \\ \pi_t \end{pmatrix} &= \begin{bmatrix} 1 & -\alpha_{y,1} & -\alpha_{y,2} \\ 0 & -\kappa & 0 \end{bmatrix} \begin{pmatrix} y_t^* \\ y_{t-1}^* \\ y_{t-2}^* \end{pmatrix} + \begin{bmatrix} \alpha_{y,1} & \alpha_{y,2} & 0 & 0 \\ \kappa & 0 & \alpha_\pi & 1-\alpha_\pi \end{bmatrix} \begin{pmatrix} y_{t-1} \\ y_{t-2} \\ \pi_{t-1} \\ \pi_{t-2|4} \end{pmatrix} + \begin{pmatrix} \varepsilon_t^{\tilde{y}} \\ \varepsilon_t^{\pi} \end{pmatrix}, \\
\begin{pmatrix} y_t^* \\ y_{t-1}^* \\ y_{t-2}^* \end{pmatrix} &= \begin{bmatrix} 1 & 0 & 0 \\ 1 & 0 & 0 \\ 0 & 1 & 0 \end{bmatrix} \begin{pmatrix} y_{t-1}^* \\ y_{t-2}^* \\ y_{t-3}^* \end{pmatrix} + \begin{bmatrix} \bar{g} \\ 0 \\ 0 \end{bmatrix} + \begin{pmatrix} \varepsilon_t^{y^*} \\ 0 \\ 0 \end{pmatrix},
\end{aligned}
$$

with variances of the disturbances in the measurement and transition equations given by

$$
\mathbf{H} = \begin{bmatrix} \sigma_{\tilde{y}}^2 & 0 \\ 0 & \sigma_\pi^2 \end{bmatrix}, \qquad \mathbf{Q} = \begin{bmatrix} \sigma_{y^*}^2 & 0 & 0 \\ 0 & 0 & 0 \\ 0 & 0 & 0 \end{bmatrix}.
$$

We initialize the filter by using values of potential output estimated by the Congressional Budget Office. To help convergence in estimation, we impose the following parameter constraints: (i) we bound the standard errors of innovations to lie in between 0 and 1; (ii) the autoregressive coefficients of the output gap are restricted to allow for stationarity: $\alpha_{y,1} + \alpha_{y,2} < 1$ and $|\alpha_{y,2}| < 1$; (iii) the autoregressive coefficient of inflation is restricted to $\alpha_\pi < 1$; and (iv) the κ parameter is restricted to be positive and satisfying the constraint $\kappa \in (0, 0.2)$ (HLW2017 estimates this parameter as 0.079).

Equations (4) and (5) form a local level model for the first difference of potential output,

$$
\begin{aligned}
\Delta y_t^* &= g_{t-1} + \varepsilon_t^{y^*} \\
g_t &= g_{t-1} + \varepsilon_t^{g}
\end{aligned}
$$

Thus, given an estimate for potential output, we can apply the Stock and Watson's (1998) median unbiased estimator of $\lambda_g = \frac{\sigma_g}{\sigma_{y^*}}$, which is obtained by computing the exponential Wald statistic of Andrews and Ploberger (1994) as in HLW2017.

Step 2: The second step consists of imposing the estimated value of λ_g from the first step, followed by the inclusion of the real interest rate gap in the output gap equation under the assumption that z_t is constant and equal to $\bar{z}$. The state-space representation of the model reads

$$\begin{pmatrix} y_t \\ \pi_t \end{pmatrix} = \begin{bmatrix} 1 & -\alpha_{y,1} & -\alpha_{y,2} & 0 & 4\gamma \\ 0 & -\kappa & 0 & 0 & 0 \end{bmatrix} \begin{pmatrix} y_t^* \\ y_{t-1}^* \\ y_{t-2}^* \\ g_t \\ g_{t-1} \end{pmatrix} +$$

$$+ \begin{bmatrix} \alpha_{y,1} & \alpha_{y,2} & 0 & 0 & -\gamma \\ \kappa & 0 & \alpha_\pi & 1-\alpha_\pi & 0 \end{bmatrix} \begin{pmatrix} y_{t-1} \\ y_{t-2} \\ \pi_{t-1} \\ \pi_{t-2|4} \\ r_{t-1} \end{pmatrix} + \begin{bmatrix} \gamma\bar{z} \\ 0 \end{bmatrix} + \begin{pmatrix} \varepsilon_t^{\tilde{y}} \\ \varepsilon_t^{\pi} \end{pmatrix},$$

$$\begin{pmatrix} y_t^* \\ y_{t-1}^* \\ y_{t-2}^* \\ g_t \\ g_{t-1} \end{pmatrix} = \begin{bmatrix} 1 & 0 & 0 & 1 & 0 \\ 1 & 0 & 0 & 0 & 0 \\ 0 & 1 & 0 & 0 & 0 \\ 0 & 0 & 0 & 1 & 0 \\ 0 & 0 & 0 & 1 & 0 \end{bmatrix} \begin{pmatrix} y_{t-1}^* \\ y_{t-2}^* \\ y_{t-3}^* \\ g_{t-1} \\ g_{t-2} \end{pmatrix} + \begin{pmatrix} \varepsilon_t^{y^*} \\ 0 \\ 0 \\ \varepsilon_t^{g} \\ 0 \end{pmatrix},$$

with variances of the disturbances in the measurement and transition equations given by

$$\mathbf{H} = \begin{bmatrix} \sigma_{\tilde{y}}^2 & 0 \\ 0 & \sigma_\pi^2 \end{bmatrix}, \qquad \mathbf{Q} = \begin{bmatrix} \sigma_{y^*}^2 & 0 & 0 & 0 & 0 \\ 0 & 0 & 0 & 0 & 0 \\ 0 & 0 & 0 & 0 & 0 \\ 0 & 0 & 0 & \lambda_g^2\sigma_{y^*}^2 & 0 \\ 0 & 0 & 0 & 0 & 0 \end{bmatrix}.$$

The ex-ante real interest rate enters in the model as exogenous variable. Following HLW2017, we construct it as the nominal interest rate net of a four-quarter moving average of past inflation. To initialize the filter we use values of CBO potential output for y^*, and values of first differences of CBO potential output for g. The variance-covariance matrix of the state vector is initialized as

$$\mathbf{P}_{0|0}^{(II)} = \begin{bmatrix} \hat{\mathbf{P}}_{T|T}^{(I)} & \mathbf{0} \\ \mathbf{0} & \mathbf{I} \end{bmatrix},$$

where $\hat{\mathbf{P}}_T^{(I)}$ is the long-run variance-covariance matrix estimated in the first step. We employ the values estimated in the previous step as initial condition for those values which have to be re-estimated. To help convergence in estimation, we impose the same parameter restrictions as in the first stage, as well as an additional restriction on γ, which imposes the parameter to be positive and satisfying the constraint $\gamma \in (0, 0.2)$. In this respect, recall that HLW2017 estimate this parameter to be equal to 0.071.

Equations (1), (3), and (6) form a local level model given by

$$
\begin{aligned}
&\tilde{y}_t - \alpha_{y,1}\tilde{y}_{t-1} - \alpha_{y,2}\tilde{y}_{t-2} + \gamma r_{t-1} - 4\gamma g_{t-1} = \gamma z_{t-1} + \varepsilon_t^{\tilde{y}} \\
&z_t = z_{t-1} + \varepsilon_t^z
\end{aligned}
$$

The Stock and Watson's (1998) median unbiased estimator of $\lambda_z = \frac{\gamma\sigma_z}{\sigma_{\tilde{y}}}$ is obtained by testing for a structural break with unknown break date by means of the exponential Wald statistics of Andrews and Ploberger (1994).

Step 3: The third and final step consists of imposing the estimated value of λ_g from the first step and λ_z from the second step, and estimating the full model by Maximum Likelihood. The measurement equation reads

$$
\begin{aligned}
\begin{pmatrix} y_t \\ \pi_t \end{pmatrix} &= \begin{bmatrix} 1 & -\alpha_{y,1} & -\alpha_{y,2} & 0 & 4\gamma & 0 & \gamma \\ 0 & -\kappa & 0 & 0 & 0 & 0 & 0 \end{bmatrix} \begin{pmatrix} y_t^* \\ y_{t-1}^* \\ y_{t-2}^* \\ g_t \\ g_{t-1} \\ z_t \\ z_{t-1} \end{pmatrix} + \\
&+ \begin{bmatrix} \alpha_{y,1} & \alpha_{y,2} & 0 & 0 & -\gamma \\ \kappa & 0 & \alpha_\pi & 1-\alpha_\pi & 0 \end{bmatrix} \begin{pmatrix} y_{t-1} \\ y_{t-2} \\ \pi_{t-1} \\ \pi_{t-2|4} \\ r_{t-1} \end{pmatrix} + \begin{pmatrix} \varepsilon_t^{\tilde{y}} \\ \varepsilon_t^{\pi} \end{pmatrix},
\end{aligned}
$$

while the transition equation reads

$$
\begin{pmatrix} y_t^* \\ y_{t-1}^* \\ y_{t-2}^* \\ g_t \\ g_{t-1} \\ z_t \\ z_{t-1} \end{pmatrix} = \begin{bmatrix} 1 & 0 & 0 & 1 & 0 & 0 & 0 \\ 1 & 0 & 0 & 0 & 0 & 0 & 0 \\ 0 & 1 & 0 & 0 & 0 & 0 & 0 \\ 0 & 0 & 0 & 1 & 0 & 0 & 0 \\ 0 & 0 & 0 & 1 & 0 & 0 & 0 \\ 0 & 0 & 0 & 0 & 0 & 1 & 0 \\ 0 & 0 & 0 & 0 & 0 & 1 & 0 \end{bmatrix} \begin{pmatrix} y_{t-1}^* \\ y_{t-2}^* \\ y_{t-3}^* \\ g_{t-1} \\ g_{t-2} \\ z_{t-1} \\ z_{t-2} \end{pmatrix} + \begin{pmatrix} \varepsilon_t^{y^*} \\ 0 \\ 0 \\ \varepsilon_t^g \\ 0 \\ \varepsilon_t^z \\ 0 \end{pmatrix}.
$$

The variances of the disturbances in the measurement and transition equations are given by

$$\mathbf{H} = \begin{bmatrix} \sigma_{\tilde{y}}^2 & 0 \\ 0 & \sigma_\pi^2 \end{bmatrix}, \qquad \mathbf{Q} = \begin{bmatrix} \sigma_{y^*}^2 & 0 & 0 & 0 & 0 & 0 & 0 \\ 0 & 0 & 0 & 0 & 0 & 0 & 0 \\ 0 & 0 & 0 & 0 & 0 & 0 & 0 \\ 0 & 0 & 0 & \lambda_g^2 \sigma_{y^*}^2 & 0 & 0 & 0 \\ 0 & 0 & 0 & 0 & 0 & 0 & 0 \\ 0 & 0 & 0 & 0 & 0 & \left(\frac{\lambda_z \sigma_{\tilde{y}}}{\gamma}\right)^2 & 0 \\ 0 & 0 & 0 & 0 & 0 & 0 & 0 \end{bmatrix}.$$

To initialize the filter we use values of CBO potential output for y^*, values of first differences of CBO potential output for g and, following HLW2017, we set to zero the initial values of the z component. The variance-covariance matrix of the state vector is initialized as

$$\mathbf{P}_{0|0}^{(III)} = \begin{bmatrix} \hat{\mathbf{P}}_{T|T}^{(II)} & \mathbf{0} \\ \mathbf{0} & \mathbf{I} \end{bmatrix},$$

where $\hat{\mathbf{P}}_T^{(II)}$ is the long-run variance-covariance matrix estimated in the second step. We employ the values estimated in the previous step as initial condition for those values which have to be re-estimated. To help convergence in estimation, we impose the same constraints on parameters as in the second step.

B Computing Confidence Bands for the State Vector

The approach closely follows Hamilton (1986). Consider the estimation of an unobserved state vector $\mathbf{x}_t$ when the true value of the parameter vector θ is unknown, given data available up to time T, $\mathbf{z}_T$. Here we take a Bayesian perspective and consider that the parameter vector is a random variable s.t. $\theta \sim N(\theta_0, \mathbf{\Sigma}_0)$. We seek to evaluate the variance of the unobserved state vector

$$E\left\{[\mathbf{x}_t - \hat{\mathbf{x}}_t(\mathbf{z}_T)]\,[\mathbf{x}_t - \hat{\mathbf{x}}_t(\mathbf{z}_T)]'\,|\mathbf{z}_T\right\}$$

which can be decomposed as

$$\begin{aligned} E\left\{[\mathbf{x}_t - \hat{\mathbf{x}}_t(\mathbf{z}_T)]\,[\mathbf{x}_t - \hat{\mathbf{x}}_t(\mathbf{z}_T)]'\,|\mathbf{z}_T\right\} &= E_{\theta|\mathbf{z}_T}\left\{[\mathbf{x}_t - \hat{\mathbf{x}}_t(\mathbf{z}_T,\theta)]\,[\mathbf{x}_t - \hat{\mathbf{x}}_t(\mathbf{z}_T,\theta)]'\,|\mathbf{z}_T\right\} + \\ &+ E_{\theta|\mathbf{z}_T}\left\{[\hat{\mathbf{x}}_t(\mathbf{z}_T,\theta) - \hat{\mathbf{x}}_t(\mathbf{z}_T)]\,[\hat{\mathbf{x}}_t(\mathbf{z}_T,\theta) - \hat{\mathbf{x}}_t(\mathbf{z}_T)]'\,|\mathbf{z}_T\right\} \end{aligned}$$

The first term in the right-hand side represents filter uncertainty, while the second term represents parameter uncertainty. To compute the filter uncertainty, generate θ_i draws, with $i = 1, \ldots, B$, of the parameter vector from a $N\left(\hat{\theta}(\mathbf{z}_T), \hat{\mathbf{\Sigma}}(\mathbf{z}_T)\right)$, where $\hat{\theta}(\mathbf{z}_T)$ is the MLE of θ and $\hat{\mathbf{\Sigma}}(\mathbf{z}_T)$ is its associated asymptotic variance-covariance matrix. For each θ_i calculate the sequences $\{\hat{\mathbf{x}}_t(\mathbf{z}_T, \theta_i)\}$ and $\left\{\hat{\mathbf{P}}_t(\mathbf{z}_T, \theta_i)\right\}$ by running through the Kalman filter. For each t, average the $\hat{\mathbf{P}}_t(\mathbf{z}_T, \theta_i)$ across draws

$$\frac{1}{B}\sum_{i=1}^{B} \hat{\mathbf{P}}_t(\mathbf{z}_T, \theta_i), \tag{18}$$

which yields a Monte Carlo estimate of the contribution of the filter uncertainty. Then, for each t calculate the variance of $\hat{\mathbf{x}}_t(\mathbf{z}_T, \theta_i)$ across draws

$$\frac{1}{B}\sum_{i=1}^{B} [\hat{\mathbf{x}}_t(\mathbf{z}_T, \theta_i) - \hat{\mathbf{x}}_t(\mathbf{z}_t)]\,[\hat{\mathbf{x}}_t(\mathbf{z}_T, \theta_i) - \hat{\mathbf{x}}_t(\mathbf{z}_t)]' \tag{19}$$

which yields an estimate of the parameter uncertainty. The estimated total variance is given by summing up the two expressions in (18) and (19). Hence, standard errors can be directly computed given the estimated variance-covariance matrices.

C Observability: Definition and Examples

Consider the general state space form in Harvey (1989) which applies to a n-variate time series observed at date t, $\mathbf{y}_t$, which contains n elements,

$$\mathbf{y}_t = \mathbf{Z}\mathbf{x}_t + \mathbf{D}\mathbf{w}_t + \mathbf{u}_t \qquad \mathbf{u}_t \sim N(\mathbf{0}, \mathbf{R}) \tag{20}$$

$$\mathbf{x}_t = \mathbf{T}\mathbf{x}_{t-1} + \mathbf{v}_t \qquad \mathbf{v}_t \sim N(\mathbf{0}, \mathbf{Q}) \tag{21}$$

where $\mathbf{x}_t$ is a $s \times 1$ vector of unobserved states, $\mathbf{w}_t$ is a $p \times 1$ vector of (observed) exogenous or predetermined variables; $\mathbf{Z}$, $\mathbf{D}$, and $\mathbf{T}$ are matrices of parameters of dimension $n \times s$, $n \times p$, and $s \times s$, respectively; $\mathbf{u}_t$ is an $n \times 1$ vector of zero-mean serially uncorrelated disturbances with covariance matrix $\mathbf{R}$; and finally $\mathbf{v}_t$ is an $s \times 1$ vector of zero-mean serially uncorrelated disturbances with covariance matrix $\mathbf{Q}$.

Suppose that the particular values of all system matrices are known with certainty. In this context, we ask the question: can we learn about the dynamic behavior of the vector of unobserved states by using information about all the observables and disturbances? The key condition which allows the state vector $\mathbf{x}_t$ to be determined exactly is that the system defined by equations (20)-(21) should be *observable*, a concept introduced in the seminal work of Kalman (1960). Following Harvey (1989, chap. 3), the linear system (20)-(21) is said to be observable if the following condition holds

$$\text{Rank} \begin{bmatrix} \mathbf{Z} \\ \mathbf{ZT} \\ \mathbf{ZT}^2 \\ \vdots \\ \mathbf{ZT}^{s-1} \end{bmatrix} = s \tag{22}$$

The key idea behind the observability condition is that the problem of determining the path of the state vector can be simplified to the problem of finding the initial condition $\mathbf{x}_0$: once we know it, we can recover the full path of the state variables given recursions of the transition equation in (21) and perfect knowledge of the disturbances $\mathbf{v}_t$. Suppose for simplicity that $\mathbf{y}_t$ is univariate: since the s-dimensional vector $\mathbf{x}_0$ contains s unknown components, it is expected that s observations are sufficient to determine $\mathbf{x}_0$. Take $t =$

$0, 1, \ldots, s-1$ and generate the following sequence,

$$\begin{aligned}
\mathbf{y}_0 &= \mathbf{Z}\mathbf{x}_0 + \mathbf{D}\mathbf{w}_0 + \mathbf{u}_0 \\
\mathbf{y}_1 &= \mathbf{Z}\mathbf{x}_1 + \mathbf{D}\mathbf{w}_1 + \mathbf{u}_1 = \mathbf{Z}\mathbf{T}\mathbf{x}_0 + \mathbf{Z}\mathbf{v}_1 + \mathbf{D}\mathbf{w}_1 + \mathbf{u}_1 \\
\mathbf{y}_2 &= \mathbf{Z}\mathbf{x}_2 + \mathbf{D}\mathbf{w}_2 + \mathbf{u}_2 = \mathbf{Z}\mathbf{T}^2\mathbf{x}_0 + \mathbf{Z}\mathbf{T}\mathbf{v}_1 + \mathbf{Z}\mathbf{v}_2 + \mathbf{D}\mathbf{w}_2 + \mathbf{u}_2 \\
&\vdots \\
\mathbf{y}_{s-1} &= \mathbf{Z}\mathbf{x}_{s-1} + \mathbf{D}\mathbf{w}_{s-1} + \mathbf{u}_{s-1} = \mathbf{Z}\mathbf{T}^{s-1}\mathbf{x}_0 + \sum_{j=1}^{s-1} \mathbf{Z}\mathbf{T}^{s-1-j}\mathbf{v}_j + \mathbf{D}\mathbf{w}_{s-1} + \mathbf{u}_{s-1}
\end{aligned}$$

which can also be written as

$$\begin{bmatrix} \mathbf{Z} \\ \mathbf{Z}\mathbf{T} \\ \mathbf{Z}\mathbf{T}^2 \\ \vdots \\ \mathbf{Z}\mathbf{T}^{s-1} \end{bmatrix} \mathbf{x}_0 = \begin{bmatrix} \mathbf{y}_0 \\ \mathbf{y}_1 \\ \mathbf{y}_2 \\ \vdots \\ \mathbf{y}_{s-1} \end{bmatrix} + \mathbf{\Gamma} \begin{bmatrix} \mathbf{v}_0 \\ \mathbf{v}_1 \\ \mathbf{v}_2 \\ \vdots \\ \mathbf{v}_{s-1} \end{bmatrix} + \mathbf{\Delta} \begin{bmatrix} \mathbf{w}_0 \\ \mathbf{w}_1 \\ \mathbf{w}_2 \\ \vdots \\ \mathbf{w}_{s-1} \end{bmatrix} + \begin{bmatrix} \mathbf{u}_0 \\ \mathbf{u}_1 \\ \mathbf{u}_2 \\ \vdots \\ \mathbf{u}_{s-1} \end{bmatrix} \tag{23}$$

where $\mathbf{\Gamma}$ and $\mathbf{\Delta}$ are $s \times s^2$ and $s \times ps$ matrices, respectively, which depend on $\mathbf{Z}$, $\mathbf{T}$, and $\mathbf{D}$. Given perfect knowledge of the realizations of the observables and disturbances which enter in the right-hand-side of (23), the system contains s linear equations in s unknowns. Hence the solution to this system is unique if and only if the matrix which premultiplies $\mathbf{x}_0$, defined as the *observability matrix*, has rank equal to the number of unknowns, s. Define such a matrix by $\mathbf{O}$, then the system (23) can be compactly written as

$$\mathbf{O}\mathbf{x}_0 = \mathbf{\Psi}$$

If $\text{Rank}(\mathbf{O}) = s$, which is the case when the rank condition in equation (22) is satisfied, then the matrix $\mathbf{O}'\mathbf{O}$ is invertible, so that the unique solution to the system is given by

$$\mathbf{x}_0 = (\mathbf{O}'\mathbf{O})^{-1}\,\mathbf{O}'\mathbf{\Psi}.$$

Thus we can recover the unique path for the state vector, $\mathbf{x}_t$, given the transition equation in (21) and perfect knowledge of the disturbances $\mathbf{v}_t$. Conversely, if $\text{Rank}(\mathbf{O}) < s$, then the matrix $\mathbf{O}'\mathbf{O}$ is not invertible, and there are infinite solutions for $\mathbf{x}_0$ which satisfy the system. Hence we cannot recover a unique path for the state vector, and the model is said to be unobservable.

Notice that the $\mathbf{O}$ matrix is constructed using powers of $\mathbf{T}$ only up to $\mathbf{T}^{s-1}$. This comes from the Cayley-Hamilton theorem, according to which $\mathbf{T}^{s+j}$ for $j \geq 0$ will be a linear combination of $\mathbf{T}^0$ through $\mathbf{T}^{s-1}$, meaning that adding further powers of $\mathbf{T}$ cannot increase the rank of the observability matrix. Also notice that the matrix $\mathbf{D}$, associated to the coefficients of the exogenous variables, does not affect the observability matrix, and hence does not alter the observability properties of the system.

To fix ideas, in the following we consider the observability properties of some simple state space models.

C.1 Local Level Model

Consider a local level model as in Watson (1986), according to which a univariate observed process, y_t, is modeled as the sum of a permanent component, y_t^*, and a transitory component $\tilde{y}_t$,

$$\begin{aligned} y_t &= y_t^* + \tilde{y}_t \\ y_t^* &= y_{t-1}^* + \varepsilon_t^{y^*} \qquad \varepsilon_t^{y^*} \sim N(0, \sigma_{y^*}^2) \\ \tilde{y}_t &= \alpha \tilde{y}_{t-1} + \varepsilon_t^{\tilde{y}} \qquad \varepsilon_t^{\tilde{y}} \sim N(0, \sigma_{\tilde{y}}^2) \end{aligned}$$

where we allow for a serially correlated transitory component with correlation coefficient that satisfies $|\alpha| < 1$. We can think of y_t as of the output level, with y_t^* being its potential level, and $\tilde{y}_t$ the output gap. Following the general state space form in (20)-(21), we can cast the model as

$$\begin{aligned} y_t &= \underbrace{\begin{bmatrix} 1 & 1 \end{bmatrix}}_{\mathbf{Z}} \begin{bmatrix} y_t^* \\ \tilde{y}_t \end{bmatrix} \\ \begin{bmatrix} y_t^* \\ \tilde{y}_t \end{bmatrix} &= \underbrace{\begin{bmatrix} 1 & 0 \\ 0 & \alpha \end{bmatrix}}_{\mathbf{T}} \begin{bmatrix} y_{t-1}^* \\ \tilde{y}_{t-1} \end{bmatrix} + \begin{bmatrix} \varepsilon_t^{y^*} \\ \varepsilon_t^{\tilde{y}} \end{bmatrix} \end{aligned}$$

Given that there are two unobserved states, the observability matrix of this system is given by

$$\mathbf{O} = \begin{bmatrix} \mathbf{Z} \\ \mathbf{ZT} \end{bmatrix} = \begin{bmatrix} 1 & 1 \\ 1 & \alpha \end{bmatrix}$$

The model is observable if the observability matrix has full rank, which always happens given that $|\alpha| < 1$. In the particular case that $\alpha = 1$, the observability matrix is rank deficient and the model is not observable, since the observed process y_t is the sum of two nonstationary processes which cannot be separately identified.

Notice that we could have alternatively written the model according to the following state space representation,

$$\begin{aligned} y_t &= (1-\alpha)y^*_{t-1} + \alpha y_{t-1} + \varepsilon^{\tilde{y}}_t + \varepsilon^{y^*}_t \\ y^*_t &= y^*_{t-1} + \varepsilon^{y^*}_t \end{aligned}$$

where the state vector just includes y^*_{t-1}. In this case the observability matrix boils down to a scalar which equals $1-\alpha$. As before, the model is observable as long as $|\alpha| < 1$. Hence the specific choice of the state space representation does not affect the observability properties of the original model.

C.2 Local Linear Trend Model

Now consider a local linear trend model,

$$\begin{aligned} y_t &= y^*_t + \tilde{y}_t \\ y^*_t &= y^*_{t-1} + g_{t-1} + \varepsilon^{y^*}_t \qquad \varepsilon^{y^*}_t \sim N(0, \sigma^2_{y^*}) \\ g_t &= g_{t-1} + \varepsilon^g_t \qquad \varepsilon^g_t \sim N(0, \sigma^2_g) \\ \tilde{y}_t &= \alpha \tilde{y}_{t-1} + \varepsilon^{\tilde{y}}_t \qquad \varepsilon^{\tilde{y}}_t \sim N(0, \sigma^2_{\tilde{y}}) \end{aligned}$$

where we restrict the transitory component to be stationary by imposing $|\alpha| < 1$. This model implies that the process for y_t is integrated of order two, since potential output depends on trend growth, g_t, which follows a random walk. Following the state-space form in (20)-(21), we can write the model as

$$\begin{aligned} y_t &= \underbrace{\begin{bmatrix} 1 & 0 & 1 \end{bmatrix}}_{\mathbf{Z}} \begin{bmatrix} y^*_t \\ g_t \\ \tilde{y}_t \end{bmatrix} \\ \begin{bmatrix} y^*_t \\ g_t \\ \tilde{y}_t \end{bmatrix} &= \underbrace{\begin{bmatrix} 1 & 1 & 0 \\ 0 & 1 & 0 \\ 0 & 0 & \alpha \end{bmatrix}}_{\mathbf{T}} \begin{bmatrix} y^*_{t-1} \\ g_{t-1} \\ \tilde{y}_{t-1} \end{bmatrix} + \begin{bmatrix} \varepsilon^{y^*}_t \\ \varepsilon^g_t \\ \varepsilon^{\tilde{y}}_t \end{bmatrix} \end{aligned}$$

Given that the model features three unobserved states, the observability matrix of this system is given by

$$\mathbf{O} = \begin{bmatrix} \mathbf{Z} \\ \mathbf{ZT} \\ \mathbf{ZT}^2 \end{bmatrix} = \begin{bmatrix} 1 & 0 & 1 \\ 1 & 1 & \alpha \\ 1 & 2 & \alpha^2 \end{bmatrix}$$

The model meets the observability condition if Rank($\mathbf{O}$) $= 3$, which always occurs since $|\alpha| < 1$. Again, in the special case that $\alpha = 1$, it is easy to see that the first and third columns of the $\mathbf{O}$ matrix, which are associated to the y_t^* and $\tilde{y}_t$ processes, are equal. Therefore the observability matrix is rank deficient and the model is not observable because it is not possible to separately identify the potential output from the output gap.

C.3 Local Linear Trend Model with a Supply Equation

Consider the local linear trend model for output, augmented by a supply equation which relates inflation, π_t, to past realizations of the output gap,

$$\begin{aligned} y_t &= y_t^* + \tilde{y}_t \\ y_t^* &= y_{t-1}^* + g_{t-1} + \varepsilon_t^{y^*} \qquad \varepsilon_t^{y^*} \sim N(0, \sigma_{y^*}^2) \\ g_t &= g_{t-1} + \varepsilon_t^g \qquad \varepsilon_t^g \sim N(0, \sigma_g^2) \\ \tilde{y}_t &= \alpha \tilde{y}_{t-1} + \varepsilon_t^{\tilde{y}} \qquad \varepsilon_t^{\tilde{y}} \sim N(0, \sigma_{\tilde{y}}^2) \\ \pi_t &= \kappa \tilde{y}_{t-1} + \varepsilon_t^{\pi} \qquad \varepsilon_t^{\pi} \sim N(0, \sigma_{\pi}^2) \end{aligned}$$

where again we assume that $|\alpha| < 1$. This model is similar to the HLW model, with the only difference that in the latter the output gap also depends on the interest rate gap.[13] Using the state-space representation in (20)-(21), we can write the model as

$$\begin{bmatrix} y_t \\ \pi_t \end{bmatrix} = \underbrace{\begin{bmatrix} 1 & 0 & \alpha \\ 0 & 0 & -\kappa \end{bmatrix}}_{\mathbf{Z}} \begin{bmatrix} y_t^* \\ g_t \\ \tilde{y}_{t-1} \end{bmatrix} + \begin{bmatrix} \varepsilon_t^{\tilde{y}} \\ \varepsilon_t^{\pi} \end{bmatrix}$$

$$\begin{bmatrix} y_t^* \\ g_t \\ \tilde{y}_{t-1} \end{bmatrix} = \underbrace{\begin{bmatrix} 1 & 1 & 0 \\ 0 & 1 & 0 \\ 0 & 0 & \alpha \end{bmatrix}}_{\mathbf{T}} \begin{bmatrix} y_{t-1}^* \\ g_{t-1} \\ \tilde{y}_{t-2} \end{bmatrix} + \begin{bmatrix} \varepsilon_t^{y^*} \\ \varepsilon_t^{g} \\ \varepsilon_{t-1}^{\tilde{y}} \end{bmatrix}$$

[13] It is also similar in spirit to Kuttner (1994), which employs a local level model for output augmented by a supply equation.

Given that the model features three unobserved states, the observability matrix of this system is given by

$$\mathbf{O} = \begin{bmatrix} \mathbf{Z} \\ \mathbf{ZT} \\ \mathbf{ZT}^2 \end{bmatrix} = \begin{bmatrix} 1 & 0 & \alpha \\ 0 & 0 & -\kappa \\ 1 & 1 & \alpha^2 \\ 0 & 0 & -\alpha\kappa \\ 1 & 2 & \alpha^3 \\ 0 & 0 & -\alpha^2\kappa \end{bmatrix}$$

Let us consider two cases. First, suppose that $\kappa = 0$, so that the model boils down to the standard local linear trend model. In this case the observability matrix has full rank since $|\alpha| < 1$, as previously shown. Second, suppose the special case $\alpha = 1$, so that the output gap, $\tilde{y}_t$, is nonstationary. We can still uniquely determine the state vector as long as $\kappa \neq 0$. Intuitively, inflation provides valuable information for the output gap because past realizations of this variable have an effect on current inflation.

Recall that results do not change if we cast the model in a different state space representation. In particular, given the identity that defines the output gap, once we know potential output we also know the output gap. We can then simplify the representation as

$$\begin{aligned}
\begin{bmatrix} y_t \\ \pi_t \end{bmatrix} &= \underbrace{\begin{bmatrix} 1-\alpha & 1 \\ \kappa & 0 \end{bmatrix}}_{\mathbf{Z}} \begin{bmatrix} y^*_{t-1} \\ g_t \end{bmatrix} + \underbrace{\begin{bmatrix} \alpha \\ -\kappa \end{bmatrix}}_{\mathbf{D}} y_{t-1} + \begin{bmatrix} \varepsilon^{\tilde{y}}_t + \varepsilon^{y^*}_t \\ \varepsilon^{\pi}_t \end{bmatrix} \\
\begin{bmatrix} y^*_t \\ g_t \end{bmatrix} &= \underbrace{\begin{bmatrix} 1 & 1 \\ 0 & 1 \end{bmatrix}}_{\mathbf{T}} \begin{bmatrix} y^*_{t-1} \\ g_{t-1} \end{bmatrix} + \begin{bmatrix} \varepsilon^{y^*}_t \\ \varepsilon^{g}_t \end{bmatrix}
\end{aligned}$$

This representation features two unobserved states instead of three, so that the observability matrix is given by

$$\mathbf{O} = \begin{bmatrix} \mathbf{Z} \\ \mathbf{ZT} \end{bmatrix} = \begin{bmatrix} 1-\alpha & 1 \\ \kappa & 0 \\ 1-\alpha & 2-\alpha \\ \kappa & \kappa \end{bmatrix}$$

As with the previous representation, in the case that $\kappa = 0$, the system boils down to the local linear trend model and the observability matrix has full rank since $|\alpha| < 1$. Alternatively, if $\alpha = 1$, we can still allow for the model to be observed as long as $\kappa \neq 0$, as previously discussed.

It is important to stress that by adding predetermined or exogenous explanatory variables in the model, results on observability do not change. For instance, let us augment the supply equation by adding predetermined variables and consider the Phillips curve employed in HLW2017,

$$\pi_t = \alpha_\pi \pi_{t-1} + (1-\alpha_\pi)\pi_{t-2,4} + \kappa \tilde{y}_{t-1} + \varepsilon_t^\pi$$

which states that the observed inflation rate depends on its own lag, on the average of its second to fourth lags, and on the lagged output gap. The model can be cast as

$$\begin{aligned}
\begin{bmatrix} y_t \\ \pi_t \end{bmatrix} &= \underbrace{\begin{bmatrix} 1-\alpha & 1 \\ \kappa & 0 \end{bmatrix}}_{\mathbf{Z}} \begin{bmatrix} y^*_{t-1} \\ g_t \end{bmatrix} + \underbrace{\begin{bmatrix} \alpha & 0 & 0 \\ -\kappa & \alpha_\pi & 1-\alpha_\pi \end{bmatrix}}_{\mathbf{D}} \begin{bmatrix} y_{t-1} \\ \pi_{t-1} \\ \pi_{t-2|4} \end{bmatrix} + \begin{bmatrix} \varepsilon_t^{\tilde{y}} + \varepsilon_t^{y^*} \\ \varepsilon_t^\pi \end{bmatrix} \\
\begin{bmatrix} y^*_t \\ g_t \end{bmatrix} &= \underbrace{\begin{bmatrix} 1 & 1 \\ 0 & 1 \end{bmatrix}}_{\mathbf{T}} \begin{bmatrix} y^*_{t-1} \\ g_{t-1} \end{bmatrix} + \begin{bmatrix} \varepsilon_t^{y^*} \\ \varepsilon_t^g \end{bmatrix}
\end{aligned}$$

We can see that the observability matrix does not change, and it is still given by

$$\mathbf{O} = \begin{bmatrix} \mathbf{Z} \\ \mathbf{ZT} \end{bmatrix} = \begin{bmatrix} 1-\alpha & 1 \\ \kappa & 0 \\ 1-\alpha & 2-\alpha \\ \kappa & \kappa \end{bmatrix}$$

Hence the addition of predetermined or exogenous observed variables does not change the observability properties of the model.

D Additional Results on Observability

D.1 Full HLW Model

Here we study the observability of the HLW model in which two lags of the output gap enter in the IS curve as in the original specification of HLW2017. The measurement equation can be written as

$$\begin{bmatrix} y_t \\ \pi_t \end{bmatrix} = \underbrace{\begin{bmatrix} 1-\alpha_{y,1} & -\alpha_{y,2} & 1+4\gamma & \gamma \\ -\kappa & 0 & 0 & 0 \end{bmatrix}}_{\mathbf{Z}} \begin{bmatrix} y^*_{t-1} \\ y^*_{t-2} \\ g_{t-1} \\ z_{t-1} \end{bmatrix} +$$

$$+ \underbrace{\begin{bmatrix} \alpha_{y,1} & \alpha_{y,2} & 0 & 0 & -\gamma \\ \kappa & 0 & \alpha_\pi & 1-\alpha_\pi & 0 \end{bmatrix}}_{\mathbf{D}} \begin{bmatrix} y_{t-1} \\ y_{t-2} \\ \pi_{t-1} \\ \pi_{t-2|4} \\ r_{t-1} \end{bmatrix} + \begin{bmatrix} \varepsilon^{\tilde{y}}_t + \varepsilon^{y^*}_t \\ \varepsilon^\pi_t \end{bmatrix}$$

The transition equation reads

$$\begin{bmatrix} y^*_t \\ y^*_{t-1} \\ g_t \\ z_t \end{bmatrix} = \underbrace{\begin{bmatrix} 1 & 0 & 1 & 0 \\ 1 & 0 & 0 & 0 \\ 0 & 0 & 1 & 0 \\ 0 & 0 & 0 & 1 \end{bmatrix}}_{\mathbf{T}} \begin{bmatrix} y^*_{t-1} \\ y^*_{t-2} \\ g_{t-1} \\ z_{t-1} \end{bmatrix} + \begin{bmatrix} \varepsilon^{y^*}_t \\ 0 \\ \varepsilon^g_t \\ \varepsilon^z_t \end{bmatrix}$$

Given that the representation features four states, the observability matrix reads

$$\mathbf{O} = \begin{bmatrix} \mathbf{Z} \\ \mathbf{ZT} \\ \mathbf{ZT}^2 \\ \mathbf{ZT}^3 \end{bmatrix} = \begin{bmatrix} 1-\alpha_{y,1} & -\alpha_{y,2} & 1+4\gamma & \gamma \\ -\kappa & 0 & 0 & 0 \\ 1-\alpha_{y,1}-\alpha_{y,2} & 0 & 2+4\gamma-\alpha_{y,1} & \gamma \\ -\kappa & 0 & -\kappa & 0 \\ 1-\alpha_{y,1}-\alpha_{y,2} & 0 & 3+4\gamma-2\alpha_{y,1}-\alpha_{y,2} & \gamma \\ -\kappa & 0 & -2\kappa & 0 \\ 1-\alpha_{y,1}-\alpha_{y,2} & 0 & 4+4\gamma-3\alpha_{y,1}-2\alpha_{y,2} & \gamma \\ -\kappa & 0 & -3\kappa & 0 \end{bmatrix}$$

Let us specialize to two cases:

Case 1. The IS curve is flat ($\gamma = 0$)

If the elasticity of current output gap to past real interest rate gap is zero, then the IS curve is completely flat. The observability matrix reads

$$\mathbf{O} = \begin{bmatrix} 1-\alpha_{y,1} & -\alpha_{y,2} & 1 & 0 \\ -\kappa & 0 & 0 & 0 \\ 1-\alpha_{y,1}-\alpha_{y,2} & 0 & 2-\alpha_{y,1} & 0 \\ -\kappa & 0 & -\kappa & 0 \\ 1-\alpha_{y,1}-\alpha_{y,2} & 0 & 3-2\alpha_{y,1}-\alpha_{y,2} & 0 \\ -\kappa & 0 & -2\kappa & 0 \\ 1-\alpha_{y,1}-\alpha_{y,2} & 0 & 4-3\alpha_{y,1}-2\alpha_{y,2} & 0 \\ -\kappa & 0 & -3\kappa & 0 \end{bmatrix}$$

The fourth column, which is related to the z_t process, is a vector of zeros. Hence $\text{Rank}(\mathbf{O}) < 4$ and the model is not observable. The output gap is completely insensitive to the real interest rate gap, so that information about the output gap cannot help identify the z_t component which enters in the interest rate gap. As a result, we cannot uniquely identify the path of z_t and, consequently, the path of the natural interest rate.

Case 2. The Phillips curve is flat ($\kappa = 0$)

If the elasticity of current inflation to past output gap is zero, the Phillips curve is flat. The observability matrix reads

$$\mathbf{O} = \begin{bmatrix} 1-\alpha_{y,1} & -\alpha_{y,2} & 1+4\gamma & \gamma \\ 0 & 0 & 0 & 0 \\ 1-\alpha_{y,1}-\alpha_{y,2} & 0 & 2+4\gamma-\alpha_{y,1} & \gamma \\ 0 & 0 & 0 & 0 \\ 1-\alpha_{y,1}-\alpha_{y,2} & 0 & 3+4\gamma-2\alpha_{y,1}-\alpha_{y,2} & \gamma \\ 0 & 0 & 0 & 0 \\ 1-\alpha_{y,1}-\alpha_{y,2} & 0 & 4+4\gamma-3\alpha_{y,1}-2\alpha_{y,2} & \gamma \\ 0 & 0 & 0 & 0 \end{bmatrix}$$

The first, second, and fourth columns are linearly dependent, being the fourth column equal to the sum of the first and second columns, multiplied by $\frac{\gamma}{1-\alpha_{y,1}-\alpha_{y,2}}$. Hence $\text{Rank}(\mathbf{O}) < 4$ and the model is not observable. Inflation is insensitive to the output gap, and the model cannot separately identify the z_t component from potential output.

D.2 Stationary z_t Process

Consider the HLW model in the case that z_t follows a stationary $AR(1)$ process,

$$z_t = \alpha_z z_{t-1} + \varepsilon_t^z$$

where $|\alpha_z| < 1$. The measurement equation remains unchanged,

$$\begin{bmatrix} y_t \\ \pi_t \end{bmatrix} = \underbrace{\begin{bmatrix} 1-\alpha_y & 1+4\gamma & \gamma \\ -\kappa & 0 & 0 \end{bmatrix}}_{\mathbf{Z}} \begin{bmatrix} y^*_{t-1} \\ g_{t-1} \\ z_{t-1} \end{bmatrix} + \underbrace{\begin{bmatrix} \alpha_y & 0 & 0 & -\gamma \\ \kappa & \alpha_\pi & 1-\alpha_\pi & 0 \end{bmatrix}}_{\mathbf{D}} \begin{bmatrix} y_{t-1} \\ \pi_{t-1} \\ \pi_{t-2|4} \\ r_{t-1} \end{bmatrix} + \begin{bmatrix} \varepsilon^{\tilde{y}}_t + \varepsilon^{y^*}_t \\ \varepsilon^\pi_t \end{bmatrix}$$

while the transition equation now reads

$$\begin{bmatrix} y^*_t \\ g_t \\ z_t \end{bmatrix} = \underbrace{\begin{bmatrix} 1 & 1 & 0 \\ 0 & 1 & 0 \\ 0 & 0 & \alpha_z \end{bmatrix}}_{\mathbf{T}} \begin{bmatrix} y^*_{t-1} \\ g_{t-1} \\ z_{t-1} \end{bmatrix} + \begin{bmatrix} \varepsilon^{y^*}_t \\ \varepsilon^g_t \\ \varepsilon^z_t \end{bmatrix}$$

The observability matrix reads

$$\mathbf{O} = \begin{bmatrix} \mathbf{Z} \\ \mathbf{ZT} \\ \mathbf{ZT}^2 \end{bmatrix} = \begin{bmatrix} 1-\alpha_y & 1+4\gamma & \gamma \\ -\kappa & 0 & 0 \\ 1-\alpha_y & 2+4\gamma-\alpha_y & \alpha_z\gamma \\ -\kappa & -\kappa & 0 \\ 1-\alpha_y & 3+4\gamma-2\alpha_y & \alpha_z^2\gamma \\ -\kappa & -2\kappa & 0 \end{bmatrix}$$

Now consider the previous two cases:

Case 1. The IS curve is flat ($\gamma = 0$)

If the elasticity of current output gap to past real interest rate gap is zero, the observability matrix reads

$$\mathbf{O} = \begin{bmatrix} 1-\alpha_y & 1 & 0 \\ -\kappa & 0 & 0 \\ 1-\alpha_y & 2-\alpha_y & 0 \\ -\kappa & -\kappa & 0 \\ 1-\alpha_y & 3-2\alpha_y & 0 \\ -\kappa & -2\kappa & 0 \end{bmatrix}$$

and the third column, which is associated to the z_t process, boils down to a vector of zeros. Therefore in this case $\text{Rank}(\mathbf{O}) < 3$ and the model is not observable either. In particular, we cannot recover a unique path for z_t. Still, we can uniquely determine the paths for potential output and trend growth, as long as either $\kappa \neq 0$ or $|\alpha_y| < 1$.

Case 2. The Phillips curve is flat ($\kappa = 0$)

If the elasticity of current inflation to past output gap is zero, the observability matrix reads

$$\mathbf{O} = \begin{bmatrix} 1-\alpha_y & 1+4\gamma & \gamma \\ 0 & 0 & 0 \\ 1-\alpha_y & 2+4\gamma-\alpha_y & \alpha_z\gamma \\ 0 & 0 & 0 \\ 1-\alpha_y & 3+4\gamma-2\alpha_y & \alpha_z^2\gamma \\ 0 & 0 & 0 \end{bmatrix}$$

In this case, the first and third columns are linearly dependent only if $\alpha_z = 1$. Hence, if $\alpha_z \neq 1$, $\text{Rank}(\mathbf{O}) = 3$, and the model is observable, and we can uniquely identify the paths for all elements of the state vector.

E A Panel Error Correction Model to Estimate r^*

Recall equation (9), which can be rewritten as,

$$r_t = r_t^* + \tilde{r}_t.$$

This equation states that the observed real interest rate can be decomposed into the natural rate and the interest rate gap. We can think of the natural interest rate as depending on a linear combination of n_f unobserved factors included in the F_t vector,

$$r_t^* = \beta' F_t, \tag{24}$$

where the F_t vector contains mutually uncorrelated random walk processes. Suppose that we observe a vector X_t of potentially mismeasured indicators of factors included in F_t,

$$X_t = F_t + e_t$$

and assume that measurement errors e_t are serially and mutually uncorrelated processes, with $E(e_t \tilde{r}_t) = 0$. Then, we can link the observed real interest rate to the set of indicators as

$$r_t = \beta' X_t + \varepsilon_t, \tag{25}$$

where $\varepsilon_t = \tilde{r}_t - \beta' e_t$. Given that the natural interest rate cointegrates with a set of unobserved factors by virtue of equation (24), cointegration also exists among the observed real interest rate and the indicators of the factors, according to equation (25). Moreover, without measurement error ($e_t = 0$), $\beta' F_t = r_t^*$ and the stationary disturbance ε_t coincides with the interest rate gap.

Hence a regression of the observed real interest rate on a number of plausible drivers of the natural interest rate delivers a predicted rate which should be a proxy for the linear combination of unobserved factors, $\beta' F_t$, which in turn coincides with the natural interest rate according to equation (24). Therefore, we can estimate equation (25) in its error correction form to recover a proxy for the natural interest rate. In order to assess the quality of the proxy, we can directly compare the predicted value of the regression with the natural interest rate estimated by the local level model.

By writing (25) in its error correction form,

$$\Delta r_t = -\left(r_{t-1} - \beta' X_{t-1}\right) + \beta' \Delta X_t + \varepsilon_t$$

any disequilibrium between the observed and predicted interest rates fully closes in one period. Since this assumption is rather restrictive, we may allow for the disequilibrium to get partially reabsorbed over time by extending (25) to an autoregressive distributed lag ARDL(1,1) model,

$$r_t = \alpha_0 + \alpha_1 r_{t-1} + \beta_0' X_t + \beta_1' X_{t-1} + \varepsilon_t$$

where for generality we have added the constant term α_0. To simplify the exposition, assume that X_t is univariate, and rearrange the equation in its error-correction form

$$\Delta r_t = -(1-\alpha_1)\left(r_{t-1} - \frac{\alpha_0}{1-\alpha_1} - \frac{\beta_0+\beta_1}{1-\alpha_1} X_{t-1}\right) + \beta_0 \Delta X_t + \varepsilon_t, \tag{26}$$

where the loading coefficient of the error-correction term is given by $-(1-\alpha_1)$: if the coefficient equals zero, no cointegration exists; if instead $-(1-\alpha_1) \in (-1, 0)$, there exists cointegration and the disequilibrium only gets partially reabsorbed in one period; finally, if $-(1-\alpha_1) = -1$, we have full error correction in one period. The idea is to estimate equation (26) to recover the loading and cointegration coefficients, and hence the predicted natural interest rate. To better identify the parameters of the relationship we exploit the cross-country variation in the data and estimate (26) in a Panel setting,

$$\Delta r_{i,t} = -(1-\alpha_1)\left(r_{i,t-1} - \frac{\alpha_{i,0}}{1-\alpha_1} - \frac{\beta_0+\beta_1}{1-\alpha_1} X_{i,t-1}\right) + \beta_0 \Delta X_{i,t} + \varepsilon_{i,t} \tag{27}$$

which improves the precision of estimates by imposing cross-country homogeneity of the loading and cointegration coefficients, while the intercept is allowed to be country-specific to allow for some heterogeneity.

F Other Tables and Figures

Table 2: Holston, Laubach, and Williams model: parameter estimates

Parameter	This paper	HLW2017
λ_g	0.043	0.053
λ_z	0.013	0.030
$\sum \alpha_y$	0.950	0.942
γ	0.048	0.071
	(3.370)	(4.063)
κ	0.096	0.079
	(2.705)	(3.136)
$\sigma_{\tilde{y}}$	0.261	0.354
σ_{π}	0.799	0.791
σ_{y^*}	0.625	0.575
σ_g	0.108	0.122
σ_z	0.074	0.150
$\sigma_{r^*} = \sqrt{\sigma_g^2 + \sigma_z^2}$	0.131	0.194

Notes: t statistics are in parentheses, σ_g is expressed at annual rate.

Table 3: Slopes of IS and Phillips curves: estimates in the literature

		Sensitivity of output gap to the interest rate gap ($-\gamma$)	Sensitivity of inflation to the output gap (κ)
United States	Laubach and Williams (2003)	-0.098	0.043
	Clark and Kozicki (2005)	-0.105	0.200
	Trehan and Wu (2007)	-0.130	0.260
	Garnier and Wilhelmsen (2009)	-0.180	0.103
	Kiley (2015)	-0.076	0.073
	Pescatori and Turunen (2015)	-0.060	0.150
	Holston et al. (2017)	-0.071	0.079
	Wynne and Zhang (2017)	-0.107	0.035
	Juselius et al. (2018)	-0.037	0.015
Euro area	Mesonnier and Renne (2007)	-0.190	0.160
	Garnier and Wilhelmsen (2009)	-0.056	0.051
	Holston et al. (2017)	-0.036	0.065
Canada	Berger and Kempa (2014)	-0.030	0.220
	Holston et al. (2017)	-0.067	0.044
Denmark	Pedersen (2015)	-0.400	0.010
Germany	Garnier and Wilhelmsen (2009)	-0.172	0.041
Japan	Wynne and Zhang (2017)	-0.043	0.532
South Africa	Kuhn et al. (2017)	-0.032	0.235
United Kingdom	Holston et al. (2017)	-0.009	0.490
World	Wynne and Zhang (2018)	-0.035	0.159

Notes: in Kiley (2015), κ measures the sensitivity of inflation to a measure of unemployment gap.

Figure 18: Filter and parameter uncertainty of U.S. r^*: HLW and local level models

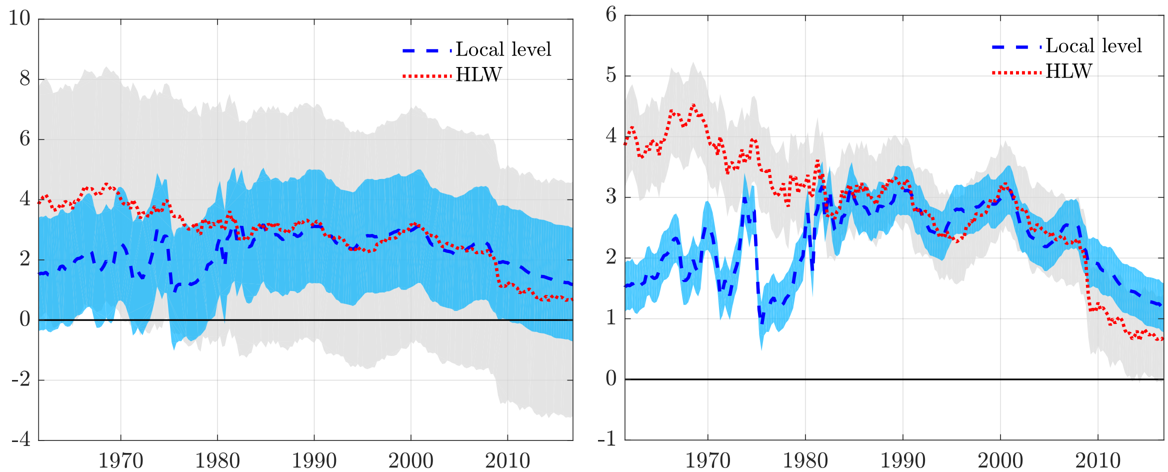

(a) Filter uncertainty (b) Parameter uncertainty

Notes: quarterly data, 1961Q2-2016Q3. Solid blue line refers to r^* estimated by the local level model. Dotted red line refers to r^* estimated by the HLW model. Panel (a) reports 90% confidence bands which reflect filter uncertainty; panel (b) reports 90% confidence bands which reflect parameter uncertainty. Bands are computed using Hamilton's (1986) approach with 2000 replications on the parameter vector.

Figure 19: Nominal interest rates, inflation, and inflation expectations across countries

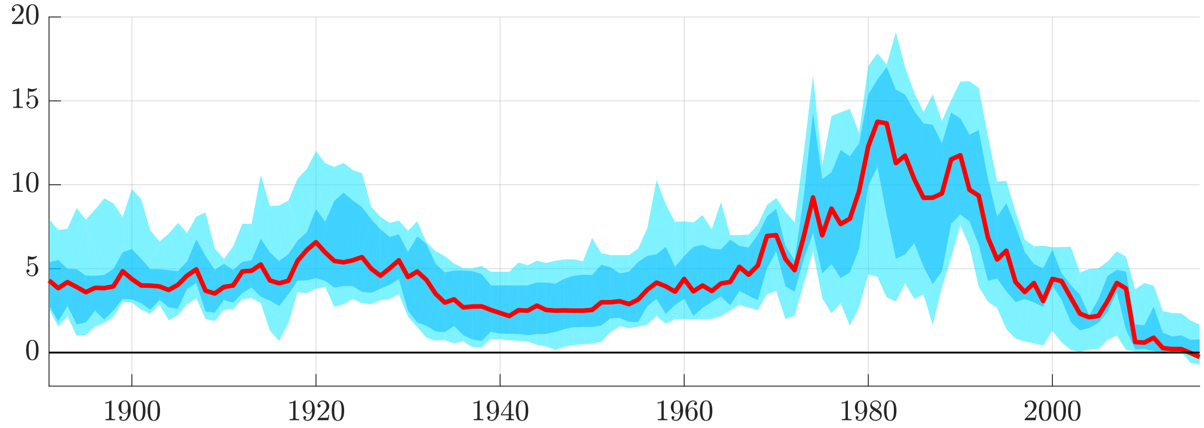

(a) Nominal short-term interest rate

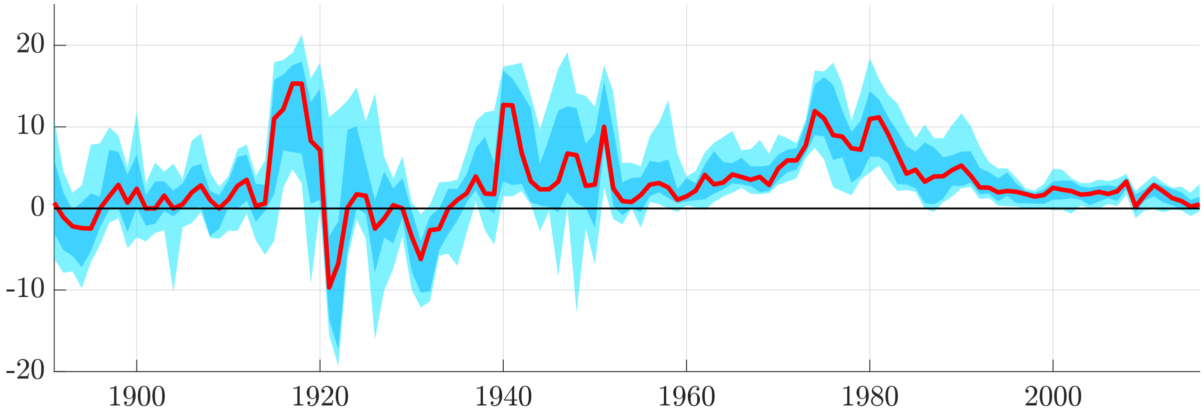

(b) Inflation rate

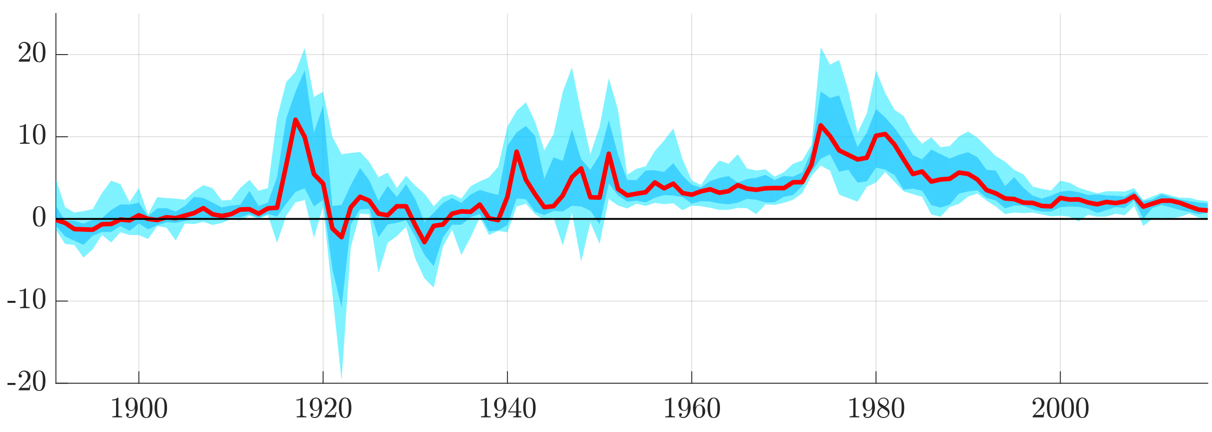

(c) Inflation expectations

Notes: annual data, 1891-2016. Cross-country median in red, 68% and 90% bands in dark and light blue, respectively. Data on nominal short-term interest rate and CPI inflation rate come from the Jordà-Schularick-Taylor (2017) Macrohistory Database and OECD Main Economic Indicators. Measures of inflation expectations are constructed by estimating a sequence of first-order autoregressive models on realized inflation with rolling twenty-years windows.

Figure 20: Estimated natural rates across countries

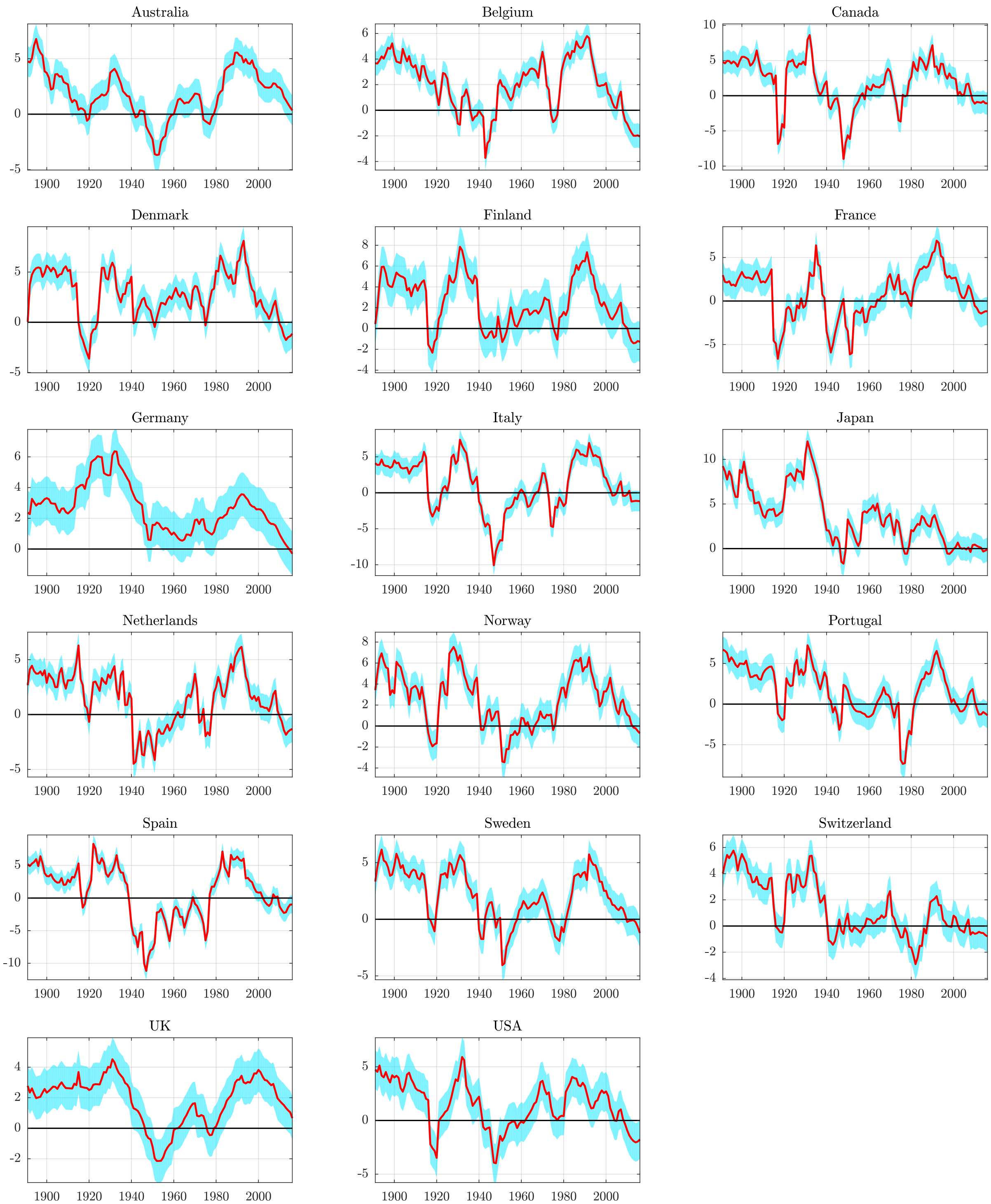

Notes: annual data, 1891-2016. Estimated r^* with 90% confidence bands. Bands reflect both filter and parameter uncertainty, following Hamilton's (1986) approach with 2000 replications on the parameter vector.

Figure 21: Estimated volatilities

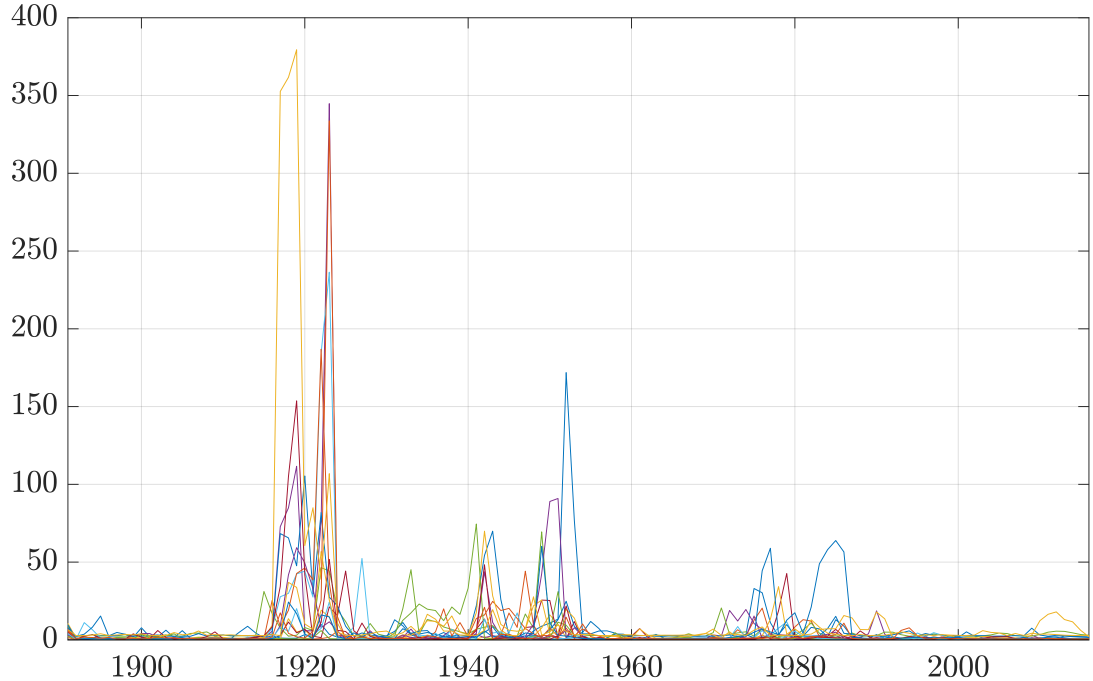

Notes: annual data, 1891-2016, for 17 economies.

Figure 22: Estimated r^* by Panel ECM and local level model

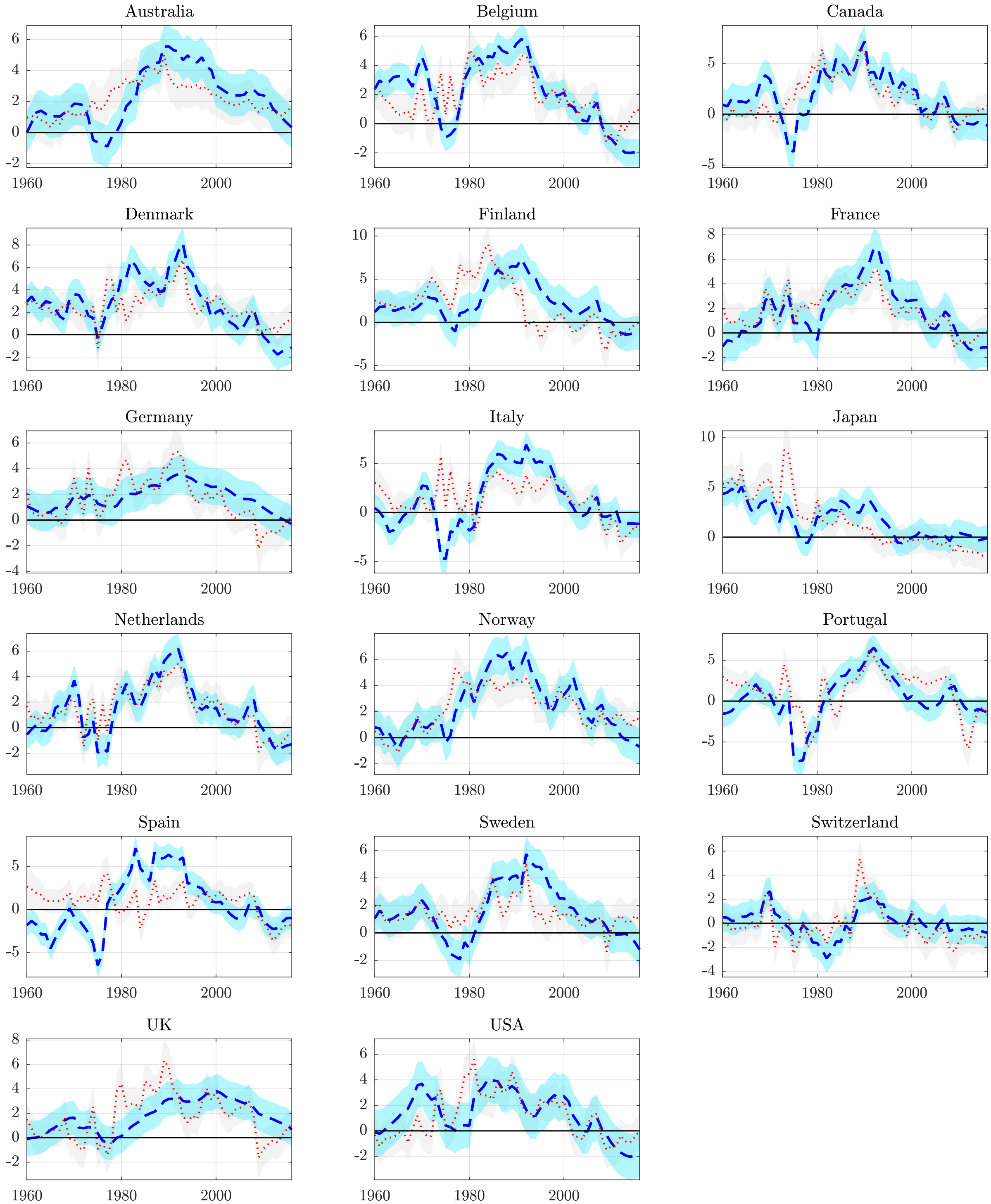

Notes: annual data, 1960-2016. Local level model estimates in dashed blue jointly with 90% confidence bands, Panel ECM estimates in dotted red jointly with 90% confidence bands.